olefin of Tam are crucial for ER binding activity.[13] So, we considered that more symmetrical derivatives of Tam might show reduced ER-binding ability.

Among our synthesized compounds, we found two, compounds **1** (YAK01) and **3** (YAK037), with potent L-Glu transporter-inhibitory activity. Studies of their mechanisms of action indicated that, unlike Tam, compound **3** acts through an ER-independent and MAPK-independent, but PI3K-dependent pathway and shows no transactivation activity for nERs. We believe this compound may represent a new platform for developing novel L-Glu transporter inhibitors with higher brain transfer rates and reduced adverse effects.

RESULTS AND DISCUSSION

We synthesized several Tam-inspired compounds bearing identical substituents on one carbon atom of the olefin,[12] and found that two of them were potent inhibitors of astrocyte L-Glu transporters. The diethyl-substituted derivative **1** inhibited L-Glu transporters in the picomolar range (62.7 ± 7.48% of control at 1 pM; Figure 2A). The dose–response curve for the inhibitory activity was not linear, but followed an inverted U-shaped curve; however, such a non-monotonic dose dependence is rather common for hormones and their mimetics.[14] On the other hand, when the symmetrical substituent was changed from ethyl to benzyl (**2**), the inhibitory effect was lost (Figure 2B). However, when the phenolic oxygen atom of **1** was substituted with a *N*,*N*-dimethylaminoethyl group (Figure 1C), we found

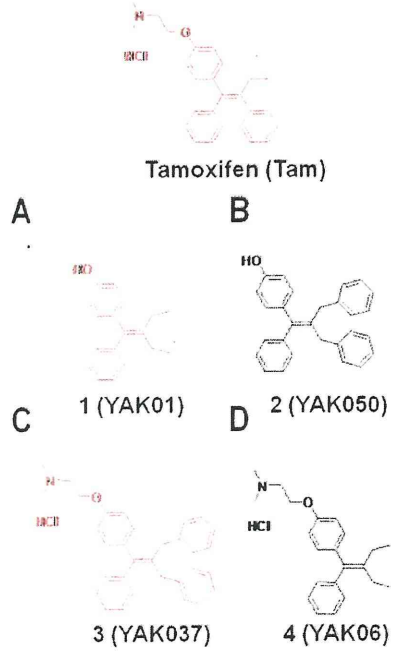

Figure 1. Chemical structures of the newly synthesized tamoxifen-related compounds.

that the resulting compound **3** showed dose-dependent L-Glu transporter inhibition in the picomolar range (63.8 ± 5.49% of control at 1 pM; Figure 2C). The dose-dependency of the effect of **3** suggested that the underlying mechanism might be different from that in the case of **1**. Compound **4** was inactive (Figure 2D).

We next examined the effects of **1** and **3** on cell viability by means of MTT reduction assay and LDH leakage assay, using the same cultured sample. Neither of the compounds was cytotoxic at concentrations below 1 μM (Figure 3), though 100 μM **1** and 10 μM **3** caused severe cell damage. These results exclude the possibility that the L-Glu clearance-inhibitory effects of these compounds at concentrations below 1 μM were caused by cell damage.

In order to confirm the involvement of L-Glu transporters in the inhibition of L-Glu uptake by our compounds, and to rule out the possibility that **1** and **3** act by inducing L-Glu release from astrocytes, we next examined the effect of **1** and **3** on L-Glu clearance when the L-Glu transporter activity was blocked with TBOA, a potent nonselective L-Glu transporter inhibitor (IC_{50}: 48 μM for GLAST/EAAT1, 7 μM for GLT1/EAAT2). We confirmed that application of 1 mM TBOA potently inhibited L-Glu transporter activity; that is, TBOA caused reversible chemical knock-down of L-Glu transporter activity.[7] When either **1** or **3** was coapplied with 1 mM TBOA, these compounds no longer influenced L-Glu clearance (Figure 4), indicating that the actions of these compounds are indeed mediated by L-Glu transporters, and do not involve L-Glu release from astrocytes.

Our cultured astrocytes predominantly expressed ERα, and little or no expression of ERβ was detected.[5] Tam is known to be a partial agonist of ERs,[9] raising the possibility that the compounds exerted their inhibitory effects via interaction with ERα. Therefore, we examined the involvement of ERα by coapplication of ICI182,780, a high-affinity antagonist of ERs. ICI182,780 dose-dependently blocked the inhibition of L-Glu uptake caused by **1** (Figure 5A) at 0.01, 0.1, and 1 μM, at which the effects of Tam were reported to be completely suppressed.[7] In contrast, ICI182,780 had no effect on the inhibition by **3** (Figure 5B), suggesting that the mechanism of the inhibition by **3** is independent of ERs. We further examined the signal transduction pathways mediating the effects of **1** and **3**. When coapplied with U0126, which inhibits mitogen-activated protein kinase/extracellular signal-regulated kinase 1 (MEK1, IC50: 70 nM) and MEK2 (IC50: 60 nM), the inhibitory effect by **1** was blocked, whereas that of **3** was not (Figure 6A). On the other hand, when coapplied with LY294002, a specific phosphoinositide 3-kinase (PI3K) inhibitor (IC50: 70 nM), the inhibitory effects of both compounds were completely blocked (Figure 6B). These results suggest that PI3K is a common mediator of the effects of both compounds, whereas mitogen-activated protein kinase (MAPK) is involved only in the mechanism of inhibition by **1**.

Finally we examined the ER-agonist potency of **1** and **3**, i.e., the transcriptional effects of these compounds via human ERα and ERβ, using HEK293/hERα and HEK293/hERβ reporter cells (Figure 7). Compound **1** showed agonist activity in both of 293/hERα and 293/hERβ reporter cells, though the binding affinities were much weaker than that of E2. The EC50 values of **1** for ERα and ERβ are 30.8 nM and 10.4 nM, respectively (1.25 nM and 0.864 nM, respectively, for E2). The relative agonist activity of **1** was 66.8% of that of E2 in HEK293/hERα and 122.0% of that of E2 in HEK293/hERβ. Strikingly, **3** showed no agonist potency for ERα or ERβ. These findings strongly suggest that **3** can inhibit L-Glu transporters without interaction with ERs.

In this study, we examined the potential of Tam-related compounds to inhibit GLAST/EAAT1 and GLT1/EAAT2, which are major astrocytic L-Glu transporters in the rat

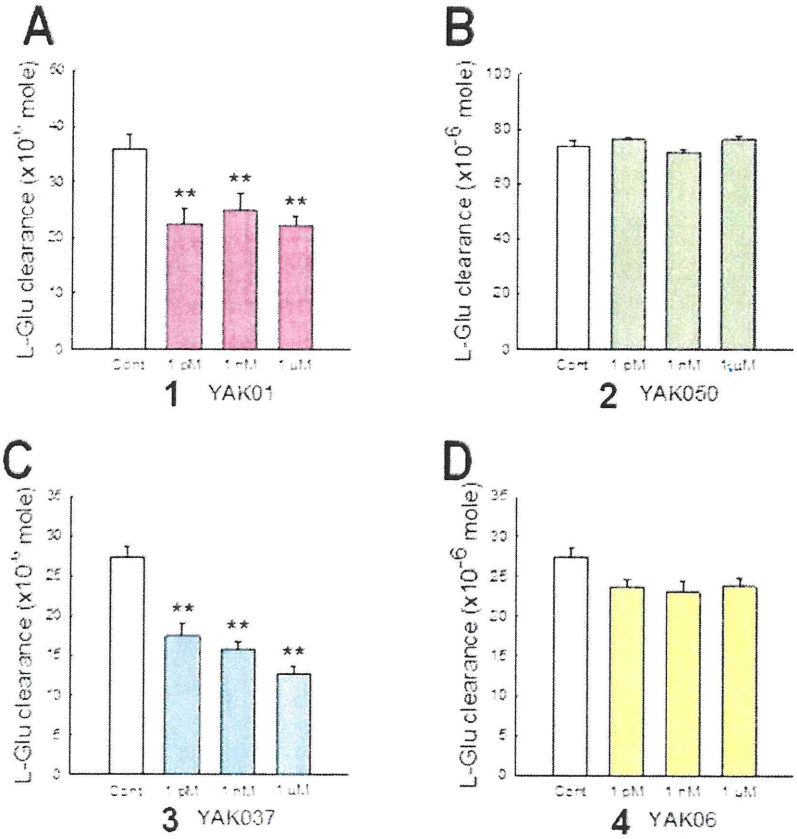

Figure 2. Compounds **1** and **3** inhibited L-Glu clearance in cultured astrocytes. The open column shows the control clearance, and colored columns show the clearance in the presence of various concentrations of compounds **1** (A), **2** (B), **3** (C), and **4** (D). $^{**}p < 0.01$ vs control group ($N = 6$), Tukey's test following ANOVA.

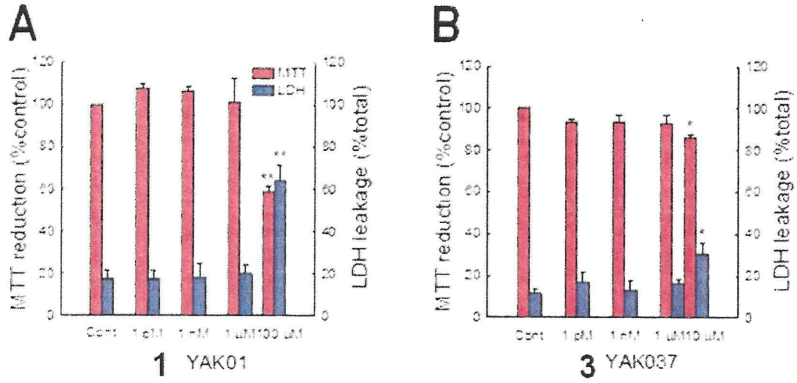

Figure 3. Effects of compounds **1** and **3** on cell viability. The results of MTT reduction and LDH leakage assays of **1** (A) and **3** (B) are shown. $^{*}p < 0.05$, $^{**}p < 0.01$ vs control group ($N = 6$), Tukey's test following ANOVA.

forebrain. Although GLT-1 is the main regulator of synaptically released L-Glu in vivo, the predominant subtype changes to GLAST in cultured astrocytes, possibly owing to the lack of interaction of astrocytes with neurons.[15] We confirmed that GLAST is the main functional L-Glu transporter in our primary-cultured astrocytes by Western blotting and pharmacological experiments (data not shown), in accordance with a previous report.[16] Therefore, the effects of the compounds observed here can be interpreted as being due to modulation of GLAST functional activity.

There is growing evidence that ERα, which is a nER that mediates genomic effects, can also be translocated to plasma membranes and mediate acute nongenomic effects in some cases. Transfection of CHO cells with nERs was reported to result in ER expression in both nuclei and membranes.[17] ERs on the plasma membranes of tumor cells were demonstrated to be structurally similar to nERs.[18] Further, mERα activated metabotropic glutamate receptor 5 (mGluR5) in striatal neurons in the CNS.[19] In our previous study, we clarified that the predominant ER subtype in cultured astrocytes was ERα, and

dx.doi.org/10.1021/cn200091w | ACS Chem. Neurosci. 2012, 3, 105–113

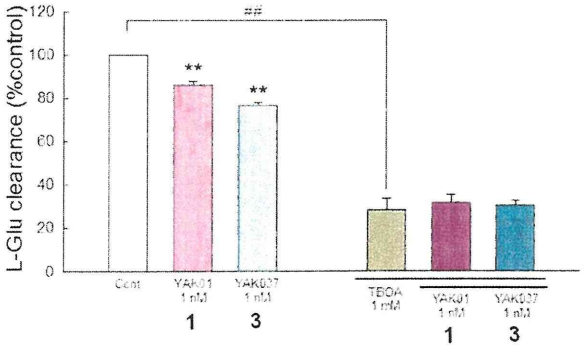

Figure 4. Compounds **1** and **3** suppressed L-Glu clearance in astrocyte culture by decreasing the functional activity of L-Glu transporter. L-Glu clearance in the presence and absence of compounds **1** and **3** is shown, together with their effects in the copresence of the potent nonselective L-Glu transporter inhibitor TBOA. $^{**}p < 0.01$ vs control group ($N = 6$), Tukey's test following ANOVA.

estrogens (such as E2 and Tam) inhibited L-Glu transporter activity via the activation of mERα.[5] We found that the effects of **1** were blocked by ICI182,780, suggesting an interaction of **1** with ERα. In addition, our pharmacological experiments showed that activation of both of MAPK and PI3K is necessary for the L-Glu transporter-inhibitory activity of **1**. There are many reports indicating that nongenomic effects involving mERα are mediated via MAPK[19−21] and PI3K.[20,22] Taken together, the effects of **1** may be mediated by mERα in a similar manner to E2 and Tam. E2 was reported to activate MAPK via both PI3K-dependent and independent pathways in a single neuron.[20] Whether or not the same signaling pathways also exist in astrocytes is not yet known. It is of interest that other studies have found that estrogens also inhibit dopamine transporter (DAT) through the activation of mERα.[23,24]

On the other hand, the effect of **3** was ER-independent and MAPK-independent, but PI3K-dependent. Our binding assay revealed that **1** binds with ERs, but **3** does not. Based on these results, we propose that the mechanisms of the L-Glu

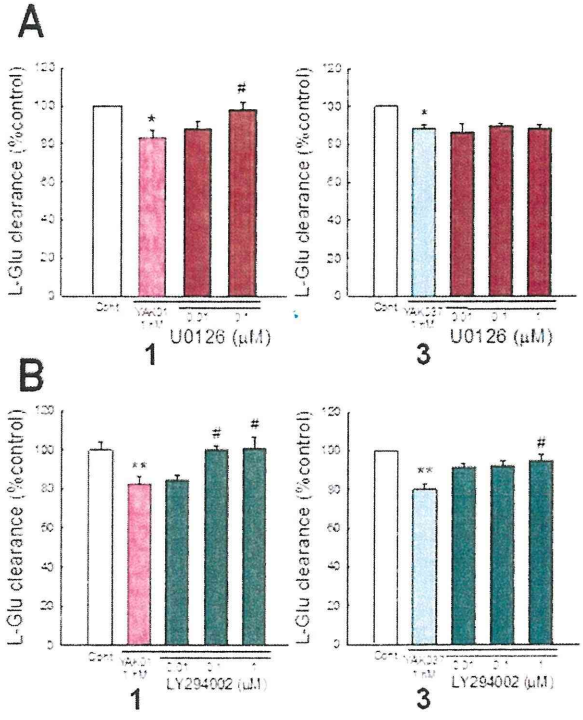

Figure 6. Involvement of MAPK and PI3K in the L-Glu transporter-inhibitory activity of compounds **1** (A) and **3** (B). Effects of compounds **1** (left panels) and **3** (right panels) on L-Glu clearance in the presence and absence of various concentrations of U0126, an inhibitor of MAPK/ERKs (A) or LY294002, a specific inhibitor of PI3K (B). $^{*}P < 0.05$, $^{**}p < 0.01$ vs control group, $\#p < 0.05$ vs compound-treated group ($N = 6$), Tukey's test following ANOVA.

transporter-inhibitory effects of **1** and **3** are different, as illustrated in Figure 8. The effect of **3** was possibly mediated by GPR30, a newly found ER, which is suggested to mediate the rapid nongenomic effects of estrogens.[25,26] In the case of GPR30, ICI182,780 acts as agonist, leading to activation of

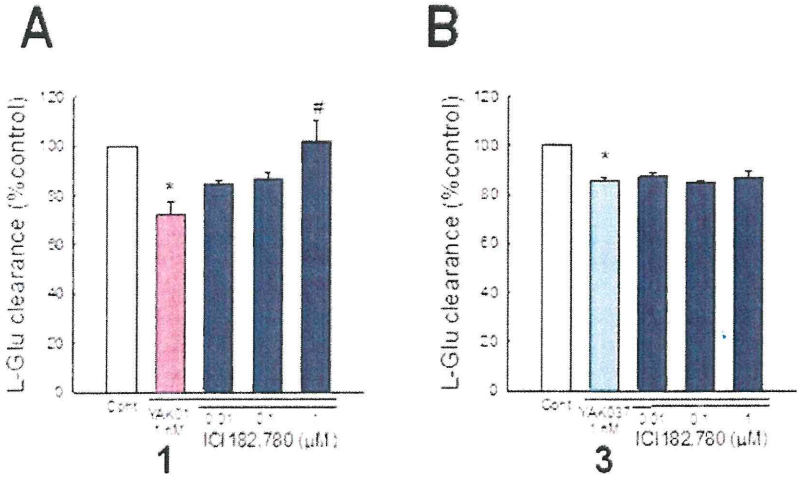

Figure 5. Involvement of ERs in the L-Glu transporter-inhibitory effects of compounds **1** and **3**. Effects of compounds **1** (A) and **3** (B) on L-Glu clearance in the presence and absence of various concentrations of ICI182,780, a high-affinity antagonist of ERs. $^{*}P < 0.05$ vs control group, $\#p < 0.05$ vs compound-treated group ($N = 6$), Tukey's test following ANOVA.

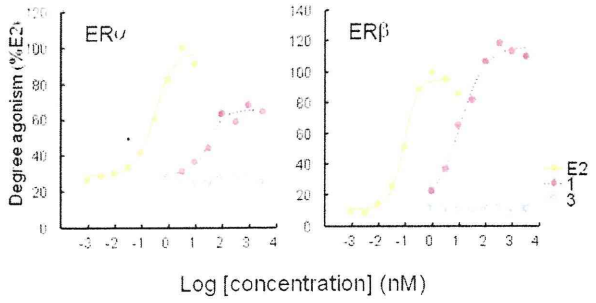

Figure 7. ER agonist potency of compounds **1** and **3** to nERs: dose dependence of binding of compounds **1** and **3** in HEK293/hERα cells (left) or HEK293/hERβ cells (right). Compound 1 showed dose-dependent agonist activity in both of HEK293/hERα cells (left) and HEK293/hERβ cells (right), though 3 showed no agonist potency for ERα or ERβ.

signal transduction pathways in a similar manner to estrogens.[27,28] However, we could not detect any effects of ICI182,780 alone on L-Glu transporter in our experiments (data not shown). In addition, Kuo et al. reported that GPR30 in astrocytes is detected not in the cell membranes but in the smooth endoplasmic reticulum,[29] while the cellular localization of GPR30 has been still controversially argued. In these contexts, GPR30 is an unlikely mediator to block the L-Glu transporters by the action of **3**.

According to Kisanga et al., the concentration of Tam in serum during conventional treatment for breast cancer (1−20 mg daily) is in the range from 20 to 225 nM.[30] Because **3** is more hydrophobic than Tam (the values of clogP for Tam and **3** are 7.56 and 9.70, respectively), it should exhibit greater permeability into the brain. Although other L-Glu transporter inhibitors, mainly L-Glu/aspartate analogues, are known, few of them have high brain transfer rates. Therefore, **3** is expected to be useful for biological research, and is also considered to be a promising candidate or lead compound for pharmacological application.

In conclusion, examination of several Tam-inspired compounds led to the discovery of two compounds that inhibited astrocytic L-Glu transporters at picomolar concentration. The inhibitory activity of compound **1** was mediated through the ER-MAPK/PI3K pathway, like that of Tam, though its transactivation activity was drastically reduced as compared with E2. In contrast, the inhibitory effect of **3** was manifested through an ER-independent and MAPK-independent, but PI3K-dependent pathway, and **3** showed no transactivation activity. These results suggest that **3** may represent a new platform for the development of novel L-Glu transporter inhibitors with higher brain transfer rates and reduced adverse effects.

METHODS

Chemistry. *General Procedures.* All reagents were commercial products and were used without further purification, unless otherwise noted. NMR data were recorded on a JEOL-400 or a Bruker Avance 400 NMR spectrometer (400 MHz for ^{1}H NMR and 100 MHz for ^{13}C NMR). *d*-$CDCl_3$ was used as a solvent, unless otherwise noted. Chemical shifts (δ) are reported in ppm with respect to internal tetramethylsilane (δ = 0 ppm) or undeuterated residual solvent (i.e., $CHCl_3$ (δ = 7.265 ppm)). Coupling constants are given in hertz. Coupling patterns are indicated as follows: m = multiplet, d = doublet, s = singlet, br = broad. High-resolution mass spectrometry (HRMS) was conducted in the electron spray ionization (ESI)-time-of-flight

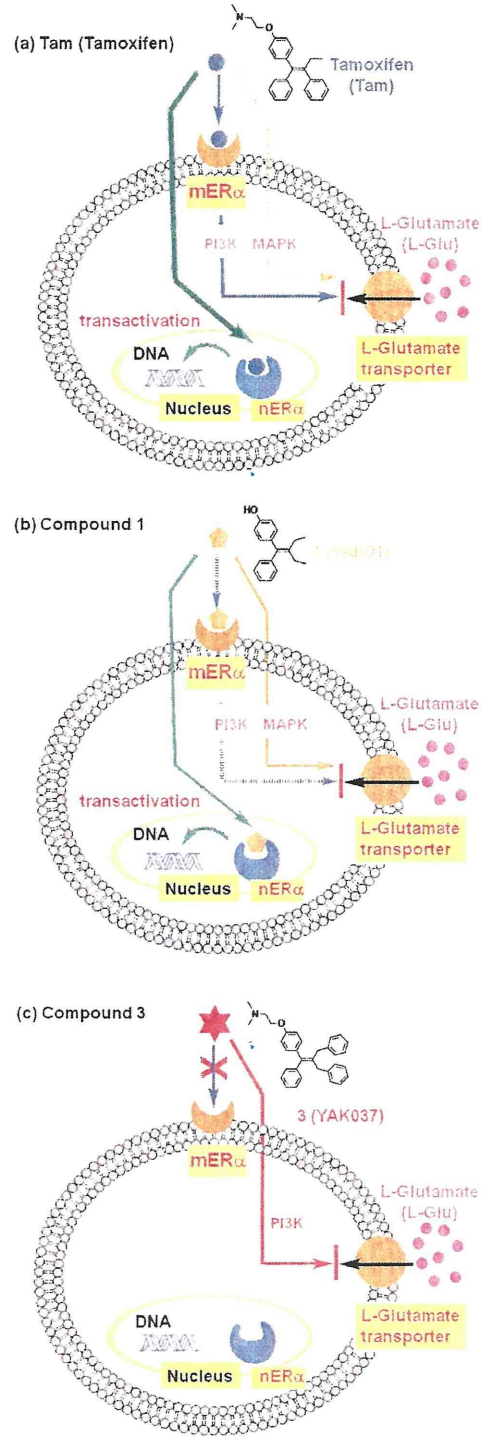

Figure 8. Schematic illustration of the proposed mechanisms of the effects of tamoxifen (a) and compounds **1** (b) and **3** (c).

(TOF) detection mode on a Bruker micrOTOF-05. FAB-MS and high-resolution FAB-MS were obtained on a JMS700-MSTATION (JEOL, Japan). Column chromatography was carried out on silica gel (silica gel 60N (100−210 μm), Kanto Chemicals, Japan). Flash column chromatography was performed on silica gel H (Merck, Germany). Analytical thin-layer chromatography (TLC) was performed on

precoated plates of silica gel HF_{254} (Merck, Germany). All the melting points were measured with a Yanaco Micro Melting Point apparatus and are uncorrected. Combustion analyses were carried out in the microanalysis laboratory of this faculty.

Synthesis of Compounds. Compounds **1** and **2** were synthesized from 4-hydroxybenzophenone and butyl-3-one or dibenzylacetone by using $TiCl_4$ in the presence of Zn. Introduction of the *N,N*-dimethylaminoethyl moiety at the phenolic hydroxyl group of **1** and **2** was carried out by base treatment, followed by addition of 2-dimethylaminoethyl chloride hydrochloride.

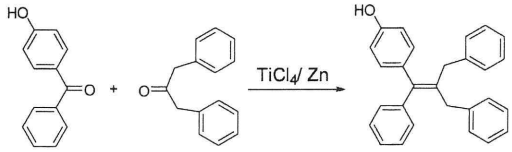

2 (YAK050)

Synthesis of Tamoxifen-Related Compounds. Compound 2 (YAK050). To a suspension of Zn powder (916.6 mg; 6.9 equiv with respect to 4-hydroxybenzophenone) in dry THF (30 mL) in a 200 mL three-necked flask, $TiCl_4$ (0.61 mL, 2.8 equiv) was added dropwise under an argon atmosphere at −20 °C (in an ice-salt bath) over 2 min. The resulting light green-yellow mixture was stirred at −20 °C for 20 min and then the cooling bath was removed. After 20 min, the flask was immersed in a preheated oil bath at 100 °C and refluxed at 100 °C with stirring for 2.5 h. To the resulting deep blue mixture was added in one portion a solution of 4-hydroxybenzophenone (401.3 mg, 2.02 mmol) and dibenzyl ketone (1.2735 g, 3 equiv) in 50 mL of dry THF. The resultant mixture was heated at reflux at 100 °C with stirring for 2 h, then allowed to cool to rt, and poured into 400 mL of 0.5 N aqueous NaOH solution. The whole was extracted with ethyl acetate (500 mL). The organic layer was washed with water, dried over $MgSO_4$ and evaporated to give a pale yellow oil (1.5172 g), which was column-chromatographed (silica gel, acetone/*n*-hexane (1:7)) to give 365.0 mg (48% yield) of the olefin **2** as a white amorphous solid. Mp: 57–60 °C. ^1H NMR ($CDCl_3$): δ: 7.287–7.079 (m, 17H), 6.760 (d, 2H, J = 8.8 Hz), 4.792 (s, 1H), 3.413 (s, 2H), 3.377 (s, 2H). ^{13}C NMR ($CDCl_3$): δ: 154.1, 143.0, 140.7, 140.4, 135.8, 135.4, 130.7, 129.4, 128.8, 128.3, 128.3, 128.2, 126.5, 125.9, 115.1, 37.4, 37.2. HRMS (ESI^-): Calcd. for $C_{28}H_{23}O$ ($[M - H]^-$), 375.1754. Found: 375.1744. Anal. Calcd for $C_{28}H_{24}O{\cdot}0.2H_2O$: C, 88.48; H, 6.47; N, 0.00. Found: C, 88.36; H, 6.63; N, 0.00.

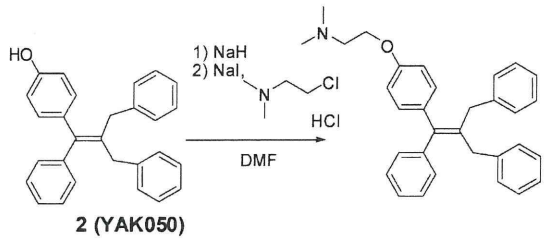

2 (YAK050)

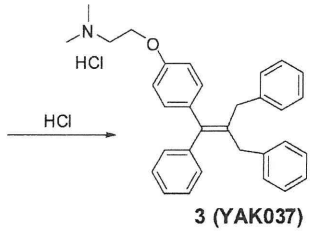

3 (YAK037)

Compound 3 (YAK037). To a suspension of NaH (60%, 42 mg, 1.05 mmol) in DMF (3 mL) at 0 °C was added a solution of the phenol **2** (158.2 mg, 0.420 mmol) in DMF (3 mL). The reaction mixture was stirred for 30 min at 0 °C, and then a solution of 2-dimethylaminoethyl chloride hydrochloride (181.0 mg, 1.256 mmol, 3.0 equiv) and NaI (94.0 mg, 0.627 mmol, 1.5 equiv) in DMF (3 mL) was added. The reaction mixture was stirred at 50 °C for 30 min, and then saturated aqueous NH_4Cl was added to quench the reaction. The mixture was extracted with Et_2O. The organic layer was washed with brine, dried over Na_2SO_4 and evaporated to afford a residue, which was column-chromatographed (ethyl acetate/Et_3N = 100/1) to give the intermediate amine (83.0 mg, 44% yield). The HCl salt of the resultant amine was prepared by repeated addition of a solution of 2 N HCl in Et_2O to a solution of the amine in ethyl acetate, followed by evaporation of the organic solvent to give **3**.

3: White solid. Mp. 169–170 °C. ^1H NMR ($CDCl_3$): δ: 13.073 (brs, 1H), 7.306–7.195 (m, 13H), 7.102–7.074 (m, 4H), 6.832 (d, 2H, J = 8.8 Hz), 4.481–4.459 (m, 2H), 3.425–3.390 (m, 6H), 2.893 (s, 6H). ^{13}C NMR ($CDCl_3$) δ: 155.7, 142.8, 140.4, 140.3, 140.2, 136.8, 136.2, 130.9, 129.4, 128.8, 128.7, 128.4, 128.3, 128.3, 126.6, 126.0, 125.9, 114.3, 62.8, 56.5, 43.6, 37.4, 37.2. HRMS (ESI^+, $[M + H]^+$): Calcd. for $C_{32}H_{34}NO$, 448.26349. Found: 448.26092. Anal. Calcd for $C_{32}H_{34}ClNO{\cdot}1/4H_2O$: C, 78.67; H, 7.12; N, 2.87. Found: C, 78.64; H, 7.30; N, 2.87.

Compound 1 (YAK01).

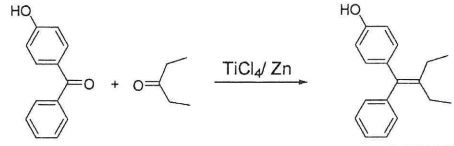

1 (YAK01)

To a suspension of Zn (0.86 g, 13.2 mmol) in 30 mL of dry THF at −5 °C was added dropwise $TiCl_4$ (0.72 mL, 6.6 mmol) under an argon atmosphere. The mixture was heated at reflux for 2 h. A solution of 4-hydroxybenzophenone (341.1 mg, 1.7 mmol) and 3-pentanone (0.50 mL, 5.0 mmol) in 50 mL of dry THF was added in one portion, and heating was continued at reflux for 6 h. Then the reaction mixture was cooled to rt, quenched with 10% aqueous K_2CO_3 (100 mL) and extracted with ethyl acetate (3 × 80 mL). The combined organic phase was washed with brine (50 mL), dried over Na_2SO_4, and evaporated to give a residue, which was flash column-chromatographed (3:1 hexane/ethyl acetate) to afford **1** (383.4 mg, 88.3%) as a white solid.

1: Mp. 76.0–76.5 °C (colorless needles, recrystallized from *n*-hexane). ^1H NMR ($CDCl_3$) δ: 7.261 (2H, t, J = 8.0 Hz), 7.173 (1H, d, J = 7.2 Hz), 7.128 (2H, d, J = 7.6 Hz), 7.009 (2H, d, J = 8.8 Hz), 6.726 (2H, d, J = 8.8 Hz), 4.763 (1H, s), 2.152 (2H, quartet, J = 7.6 Hz), 2.115 (2H, quartet, J = 6.0 Hz), 1.007 (3H, t, J = 7.6 Hz), 0.994 (3H, t, J = 7.6 Hz). ^{13}C NMR ($CDCl_3$) δ: 153.7, 143.7, 142.0, 136.5, 136.2, 130.5, 129.2, 127.9, 125.9, 114.8, 24.4, 24.3, 13.3. HRMS (ESI^-, $[M - H]^-$): Calcd. for $C_{18}H_{19}O^-$, 251.14414. Found: 251.14730. HRMS (FAB-MS, $[M]^+$) Calcd. for $C_{18}H_{20}O$, 252.1514. Found: 252.1528. Anal. Calcd. for $C_{18}H_{20}O$: C, 85.67; H, 7.99; N, 0.00. Found: C, 85.38; H, 8.13; N, 0.00.

Compound 4 (YAK06).

2-Dimethylaminoethyl chloride hydrochloride (282.4 mg, 2.0 mmol) and K_2CO_3 (1.5734 g, 11.4 mmol) were stirred in acetone/H_2O (18 mL/2 mL) at 0 °C for 30 min, then compound **1** (139.1 mg, 0.55 mmol) and K_2CO_3 (421.1 mg, 3.1 mmol) were added, and the whole was heated at reflux for 24 h, then cooled to rt. Inorganic materials were removed by filtration, and the filtrate was evaporated. The residue was flash column-chromatographed (100:1 ethyl acetate/Et_3N) to afford the amine as a white solid (88.0 mg). To a solution of the amine in ethyl acetate, a solution of HCl in ether was added to give a precipitate, which was collected and recrystallized from ethanol/ethyl acetate to give **4** (95.0 mg, 48%) as a white powder. **4**: Mp. 129.5–130.2 °C. ^1H NMR ($CDCl_3$) δ 726–6.90 (9H, m), 4.07 (2H, t, J = 6.0 Hz), 2.75 (2H, t, J = 6.0 Hz), 2.40 (6H, s), 2.15 (4H, d, J = 7.2 Hz), 1.00 (6H, t, J = 7.2 Hz). HRMS (FAB-MS, $[M\text{-}Cl]^+$): Calcd. for $C_{22}H_{30}NO^+$: 324.2322. Found: 324.2321.

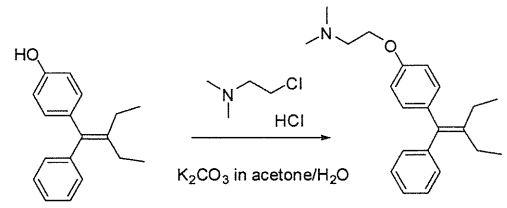

1 (YAK01)

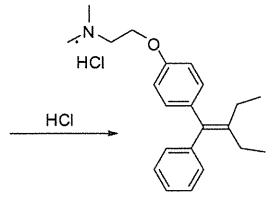

4 (YAK06)

Biology. All procedures using live animals in this study were conducted in accordance with the guidelines of the National Institute of Health Sciences, Japan.

Materials. Dulbecco's modified Eagle's medium (DMEM) and fetal bovine serum (FBS) were purchased from GIBCO (CA, USA). Glutamate dehydrogenase (GLD) was purchased from Roche (Mannheim, Germany). β-Nicotinamide adenine dinucleotide (βNAD), 3-(4,5-dimethyl-2-thiazolyl)-2,5-diphenyl-2H-tetrazolium bromide (MTT), 1-methoxy-5-methylphenazinium methyl sulfate (MPMS), lactate lithium salt and LY294002 were purchased from Sigma (MO, USA). DL-threo-β-benzyloxyaspartic acid (TBOA) and ICI182,780 were purchased from Tocris (MO, USA). U0126 was purchased from Promega (WI, USA). Assay kits for hormonal effects on HEK293/hERα and HEK293/hERβ reporter cells were purchased from Clontech (CA, USA).

Cell Culture. Primary cultures of astrocytes were prepared from the cerebral cortices of 3-day-old neonates of Wistar rats, as described previously.[31] Briefly, dissociated cortical cells were suspended in modified DMEM containing 30 mM glucose, 2 mM glutamine, 1 mM pyruvate and 10% FBS, and plated on uncoated 75 cm^2 flasks at the density of 600 000 cells/cm^2. A monolayer of type I astrocytes was obtained 12−14 days after plating. Nonastrocytes such as microglia were detached from the flasks by shaking and removed by changing the medium. Astrocytes in the flasks were dissociated by trypsinization, reseeded on uncoated 96-well microtiter plates at 20 000 cells/cm^2, and incubated until the cells became confluent (approximately 9−10 days after reseeding). In this culture, >98% of the cells were identified as type I astrocytes on the basis of positivity for GFAP and flattened, polygonal appearance.

Measurement of Extracellular L-Glu Concentration. Extracellular L-Glu concentration was measured by means of a colorimetric method according to Abe et al.[32] Briefly, 50 μL of culture supernatant was transferred to each well of a 96-well microtiter plate and mixed with 50 μL of substrate mixture consisting of 20 U/mL GLD, 2.5 mg/mL β-NAD, 0.25 mg/mL MTT, 100 μM MPMS and 0.1% (v/v) Triton X-100 in 0.2 M Tris-HCl buffer (pH 8.2). After 10 min incubation at 37 °C, the reaction was stopped by adding 100 μL of solution containing 50% (v/v) dimethylformamide and 20% (wt/vol) SDS (pH 4.7). In this reaction, MTT (yellow) is converted into MTT formazan (purple) in proportion to the L-Glu concentration. The amount of MTT formazan was determined by measuring the absorbance at 570 nm (test wavelength) and 655 nm (reference wavelength) with a microplate reader. The concentration of L-Glu was estimated from a standard curve, which was constructed in each assay using cell-free medium containing known concentrations of L-Glu. L-Glu clearance was shown as the amount of L-Glu taken up by astrocytes, which was calculated from the concentration difference in the medium.

Treatment with Test Compounds. L-Glu was dissolved at 1 mM in phosphate-buffered saline and diluted to 100 μM with the culture medium. Compounds **1**, **2**, **3**, and **4** were dissolved at 100, 100, 100, and 10 mM, respectively, in dimethyl sulfoxide (DMSO) and diluted to the required final concentrations with the culture medium. The concentration of DMSO in the medium was controlled to be below 0.1%, because we had already confirmed that 0.1% DMSO has no effect on L-Glu transport activity or cell viability (data not shown). Cells were incubated with test compounds for 24 h. TBOA (IC50 = 48 μM for GLAST, 7 μM for GLT1) was freshly dissolved at 1 mM in culture medium for each experiment. ICI182,780 (IC50 = 0.29 nM for ERs), U0126 (IC50 = 72 nM for MEK1, 58 nM for MEK2), and LY294002 (IC50 = 1 μM for class 1 PI3K, 19 μM for class 2 PI3K) were dissolved at 1, 5, and 5 mM, respectively, in DMSO, and the solutions were diluted with culture medium to yield the required final concentrations. These inhibitors were coapplied with 1 nM test compounds (**1**−**4**) for 24 h.

Assay Procedure for Hormonal Effects on HEK293/hERα and HEK293/hERβ Reporter Cells. Human embryo kidney 293 cells (HEK293) were grown in FBS (+) DMEM in 100 mm dishes. Cells were subcultured once or twice a week at about 80% confluence. A solution of 12.4 μL of 2 M calcium ion, 100 ng/well reporter or negative control vector (pERE-TA-SEAP or pTA-SEAP, Clontech), 50 ng/well expression vector (pcDNA3 ERα or pcDNA3 ERβ, generous gift from Dr. Shige-aki Kato, University of Tokyo, Japan), and 100 ng/well positive control vector (pSV-β-galactosidase, Promega) was diluted to a final volume of 10 μL/well. This mixture was carefully added dropwise to the same volume of HEPES solution with slow vortexing, and the mixture was incubated at rt for 20 min to obtain a precipitate. Cells from the exponential growth phase were seeded (3.0×10^4 cells/ml) into 96-well plates the day before transfection. The cells were incubated with fresh medium for 1 h, then 1/10 volume of precipitate was added to each well and incubation was continued for 24 h at 37 °C in an atmosphere of 5% CO_2 in air. The medium was replaced with fresh FBS (-) medium and incubation was continued for a further 24 h. Then the cells were incubated with test compounds for 24 h at 37 °C in an atmosphere of 5% CO_2 in air. SEAP activity (Great EscapeTM SEAP chemiluminescence kit 2.0, Clontech) and β-galactosidase activity (β-Galactosidase Enzyme Assay System with Reporter Lysis Buffer, Promega) were measured with a Spectramax M5 microplate reader (Molecular Devices Japan, Tokyo, Japan). All transfections were performed in triplicate.

Statistical Analysis. Data were obtained from four independent experiments (averaged values of six wells for each) unless otherwise noted. Data are expressed as means ± SEM of these data. Tests of homogeneity of variance, normality, and distribution were performed to ensure that the assumptions required for standard parametric ANOVA were satisfied. Statistical analysis was performed by one-way repeated-measures ANOVA with post hoc Tukey's test for multiple pairwise comparisons.

AUTHOR INFORMATION

Corresponding Author

*(K.S.) Telephone and Fax: +81-3-3700-9698. E-mail: kasato@nihs.go.jp. (T.O.) Telephone: +81-3-5840-4730. Fax: +81-3-5840-4735. E-mail: ohwada@mol.f.u-tokyo.ac.jp.

Author Contributions

†These two authors equally contributed to this Article. Individual author contributions: K.S. designed the biological experimental plan, performed biological experiments, data analysis, manuscript writing and preparation. J.K. and Y.S. performed experimental work. K.T. contributed to the data analysis. J.O., K.N. and Y.S. provided advice on the experimental direction. Y.O. carried out organic synthesis, data analysis and wrote portions of the manuscript. Y.S. carried out organic synthesis. T.O. designed and oversaw all organic chemistry studies, carried out organic synthesis and also performed data analysis and manuscript writing and preparation.

Funding

This work was partly supported by a Grant-in-Aid from the Food Safety Commission, Japan (No. 1003), a Grant-in-Aid for Young Scientists from MEXT, Japan (KAKENHI 21700422), the Program for Promotion of Fundamental Studies in Health Sciences of NIBIO, Japan, a Health and Labor Science Research Grant for Research on Risks of Chemicals, a Health and Labor Science Research Grant for Research on New Drug Development from MHLW, Japan, awarded to K.S., and a Health and Labor Science Research Grant for Research on Risks of Chemicals from MHLW, Japan, awarded to K.N. and T.O.

Notes

The authors declare no competing financial interest.

■ ACKNOWLEDGMENTS

We thank Dr. Shige-aki Kato for providing pcDNA3 hERα and pcDNA3 hERβ.

■ ABBREVIATIONS

βNAD; β-nicotinamide adenine dinucleotide; CNS; central nervous system; DMEM; Dulbecco's modified Eagle's medium; DMSO; dimethyl sulfoxide; E2; 17β-estradiol; ESI; electron spray ionization; FBS; fetal bovine serum; GLD; glutamate dehydrogenase; HEK-293; Human embryo kidney 293 cells; HRMS; high-resolution mass spectrometry; L-Glu; L-glutamate; MAPK; mitogen-activated protein kinase; MEK; mitogen-activated protein kinase/extracellular signal-regulated kinase; mERα; membrane-associated estrogen receptor α; mGluR5; metabotropic glutamate receptor 5; MPMS; 1-methoxy-5-methylphenazinium methyl sulfate; MTT; 3-(4,5-dimethyl-2-thiazolyl)-2,5-diphenyl-2H-tetrazolium bromide; nERs; nuclear estrogen receptors; PI3K; phosphatidylinositol 3-kinase; Tam; tamoxifen; TBOA; DL-threo-β-benzyloxyaspartic acid; TLC; thin-layer chromatography; TOF; time-of-flight

■ REFERENCES

(1) Kumar, A., Singh, R. L., and Babu, G. N. (2010) Cell death mechanisms in the early stages of acute glutamate neurotoxicity. *Neurosci. Res. 66*, 271–278.

(2) Choi, D. W. (1988) Glutamate neurotoxicity and diseases of the nervous system. *Neuron 1*, 623–634.

(3) Logan, W. J., and Snyder, S. H. (1971) Unique high affinity uptake systems for glycine, glutamic and aspartic acids in central nervous tissue of the rat. *Nature 234*, 297–299.

(4) Beart, P. M., and O'Shea, R. D. (2007) Transporters for L-glutamate: an update on their molecular pharmacology and pathological involvement. *Br. J. Pharmacol. 150*, 5–17.

(5) Sato, K., Matsuki, N., Ohno, Y., and Nakazawa, K. (2003) Estrogens inhibit L-glutamate uptake activity of astrocytes via membrane estrogen receptor alpha. *J. Neurochem. 86*, 1498–1505.

(6) Olivier, S., Close, P., Castermans, E., de Leval, L., Tabruyn, S., Chariot, A., Malaise, M., Merville, M. P., Bours, V., and Franchimont, N. (2006) Raloxifene-induced myeloma cell apoptosis: a study of nuclear factor-kappaB inhibition and gene expression signature. *Mol. Pharmacol. 69*, 1615–1623.

(7) Sato, K., Saito, Y., Oka, J., Ohwada, T., and Nakazawa, K. (2008) Effects of tamoxifen on L-glutamate transporters of astrocytes. *J. Pharmacol. Sci. 107*, 226–230.

(8) Bunch, L., Erichsen, M. N., and Jensen, A. A. (2009) Excitatory amino acid transporters as potential drug targets. *Expert Opin. Ther. Targets 13*, 719–731.

(9) Margueron, R., Duong, V., Bonnet, S., Escande, A., Vignon, F., Balaguer, P., and Cavailles, V. (2004) Histone deacetylase inhibition and estrogen receptor alpha levels modulate the transcriptional activity of partial antiestrogens. *J. Mol. Endocrinol. 32*, 583–594.

(10) Thompson, D. S., Spanier, C. A., and Vogel, V. G. (1999) The relationship between tamoxifen, estrogen, and depressive symptoms. *Breast J. 5*, 375–382.

(11) Grilli, S. (2006) Tamoxifen (TAM): the dispute goes on. *Ann. Ist. Super. Sanita 42*, 170–173.

(12) Sha, Y., Tashima, T., Mochizuki, Y., Toriumi, Y., Adachi-Akahane, S., Nonomura, T., Cheng, M., and Ohwada, T. (2005) Compounds structurally related to tamoxifen as openers of large-conductance calcium-activated K^+ channel. *Chem. Pharm. Bull. (Tokyo) 53*, 1372–1373.

(13) Robertson, D. W., Katzenellenbogen, J. A., Long, D. J., Rorke, E. A., and Katzenellenbogen, B. S. (1982) Tamoxifen antiestrogens. A comparison of the activity, pharmacokinetics, and metabolic activation of the cis and trans isomers of tamoxifen. *J. Steroid Biochem. 16*, 1–13.

(14) Weltje, L., vom Saal, F. S., and Oehlmann, J. (2005) Reproductive stimulation by low doses of xenoestrogens contrasts with the view of hormesis as an adaptive response. *Hum. Exp. Toxicol. 24* (9), 431–437.

(15) Perego, C., Vanoni, C., Bossi, M., Massari, S., Basudev, H., Longhi, R., and Pietrini, G. (2000) The GLT-1 and GLAST glutamate transporters are expressed on morphologically distinct astrocytes and regulated by neuronal activity in primary hippocampal co-cultures. *J. Neurochem. 75*, 1076–1084.

(16) Guillet, B., Lortet, S., Masmejean, F., Samuel, D., Nieoullon, A., and Pisano, P. (2002) Developmental expression and activity of high affinity glutamate transporters in rat cortical primary cultures. *Neurochem. Int. 40*, 661–671.

(17) Razandi, M., Pedram, A., Greene, G. L., and Levin, E. R. (1999) Cell membrane and nuclear estrogen receptors (ERs) originate from a single transcript: studies of ERalpha and ERbeta expressed in Chinese hamster ovary cells. *Mol. Endocrinol. 13*, 307–319.

(18) Pappas, T. C., Gametchu, B., and Watson, C. S. (1995) Membrane estrogen receptors identified by multiple antibody labeling and impeded-ligand binding. *FASEB J. 9*, 404–410.

(19) Grove-Strawser, D., Boulware, M. I., and Mermelstein, P. G. (2010) Membrane estrogen receptors activate the metabotropic glutamate receptors mGluR5 and mGluR3 to bidirectionally regulate CREB phosphorylation in female rat striatal neurons. *Neuroscience 170*, 1045–1055.

(20) Mannella, P., and Brinton, R. D. (2006) Estrogen receptor protein interaction with phosphatidylinositol 3-kinase leads to activation of phosphorylated Akt and extracellular signal-regulated kinase 1/2 in the same population of cortical neurons: a unified mechanism of estrogen action. *J. Neurosci. 26*, 9439–9447.

(21) Szego, E. M., Barabas, K., Balog, J., Szilagyi, N., Korach, K. S., Juhasz, G., and Abraham, I. M. (2006) Estrogen induces estrogen receptor alpha-dependent cAMP response element-binding protein phosphorylation via mitogen activated protein kinase pathway in basal forebrain cholinergic neurons in vivo. *J. Neurosci. 26*, 4104–4110.

(22) Vasudevan, N., Kow, L. M., and Pfaff, D. (2005) Integration of steroid hormone initiated membrane action to genomic function in the brain. *Steroids 70*, 388–396.

(23) Alyea, R. A., Laurence, S. E., Kim, S. H., Katzenellenbogen, B. S., Katzenellenbogen, J. A., and Watson, C. S. (2008) The roles of membrane estrogen receptor subtypes in modulating dopamine transporters in PC-12 cells. *J. Neurochem. 106* (4), 1525–1533.

(24) Watson, C. S., Alyea, R. A., Hawkins, B. E., Thomas, M. L., Cunningham, K. A., and Jakubas, A. A. (2006) Estradiol effects on the dopamine transporter - protein levels, subcellular location, and function. *J. Mol. Signaling 1*, 5.

(25) Filardo, E. J., and Thomas, P. (2005) GPR30: a seven-transmembrane-spanning estrogen receptor that triggers EGF release. *Trends. Endocrinol. Metab. 16* (8), 362–367.

(26) Revankar, C. M., Cimino, D. F., Sklar, L. A., Arterburn, J. B., and Prossnitz, E. R. (2005) A transmembrane intracellular estrogen receptor mediates rapid cell signaling. *Science 11;307* (5715), 1625–1630.

(27) Filardo, E. J., Quinn, J. A., Bland, K. I., and Frackelton, A. R. Jr. (2000) Estrogen-induced activation of Erk-1 and Erk-2 requires the G

protein-coupled receptor homolog, GPR30, and occurs via transactivation of the epidermal growth factor receptor through release of HB-EGF. *Mol. Endocrinol. 14* (10), 1649–1660.

(28) Thomas, P., Pang, Y., Filardo, E. J., and Dong, J. (2005) Identity of an estrogen membrane receptor coupled to a G protein in human breast cancer cells. *Endocrinology 146* (2), 624–632.

(29) Kuo, J., Hamid, N., Bondar, G., Prossnitz, E. R., and Micevych, P. (2010) Membrane estrogen receptors stimulate intracellular calcium release and progesterone synthesis in hypothalamic astrocytes. *J. Neurosci. 30* (39), 12950–12957.

(30) Kisanga, E. R., Gjerde, J., Guerrieri-Gonzaga, A., Pigatto, F., Pesci-Feltri, A., Robertson, C., Serrano, D., Pelosi, G., Decensi, A., and Lien, E. A. (2004) Tamoxifen and metabolite concentrations in serum and breast cancer tissue during three dose regimens in a randomized preoperative trial. *Clin. Cancer Res. 10*, 2336–2343.

(31) Suzuki, K., Ikegaya, Y., Matsuura, S., Kanai, Y., Endou, H., and Matsuki, N. (2001) Transient upregulation of the glial L-glutamate transporter GLAST in response to fibroblast growth factor, insulin-like growth factor and epidermal growth factor in cultured astrocytes. *J. Cell Sci. 114*, 3717–3725.

(32) Abe, K., Abe, Y., and Saito, H. (2000) Evaluation of L-glutamate clearance capacity of cultured rat cortical astrocytes. *Biol. Pharm. Bull. 23*, 204–207.

Toxicology Letters 206 (2011) 172–177

Contents lists available at ScienceDirect

Toxicology Letters

journal homepage: www.elsevier.com/locate/toxlet

Time-dependent variation in the biodistribution of C_{60} in rats determined by liquid chromatography–tandem mass spectrometry

Reiji Kubota[a,*], Maiko Tahara[a], Kumiko Shimizu[a], Naoki Sugimoto[a], Akihiko Hirose[b], Tetsuji Nishimura[a]

[a] Division of Environmental Chemistry, National Institute of Health Sciences, Kamiyoga 1-18-1, Setagaya-ku, Tokyo 158-8501, Japan
[b] Division of Risk Assessment, Biological Safety Research Center, National Institute of Health Sciences, Kamiyoga 1-18-1, Setagaya-ku, Tokyo 158-8501, Japan

ARTICLE INFO

Article history:
Received 7 June 2011
Received in revised form 8 July 2011
Accepted 8 July 2011
Available online 20 July 2011

Keywords:
Fullerenes
Tissue distribution
Rat
LC–MS/MS
Nanoparticles

ABSTRACT

We examined the biodistribution of C_{60} in rats after tail vein administration using LC–MS/MS. C_{60} was detected in various tissues, such as brain, kidneys, liver, lungs, and spleen of rats. On the other hand, no C_{60} was found in blood. The highest C_{60} concentration was observed in the lungs, followed by spleen, liver, kidneys, and brain. These results suggested that C_{60} injected in the tail vein could be filtered by lung capillary vessels and accumulate in the lungs prior to being distributed to other tissues. Moreover, C_{60} not being detected in the blood indicates that clearance of C_{60} from the blood by filtration might effectively occur in the lungs. The time-dependent variation in the biodistribution of C_{60} was evaluated. A time-dependent decrease in C_{60} concentrations was observed in all tissues, except spleen. Moreover, a decreasing trend of C_{60} levels differed among tissues, which could be due to differences in accumulation. These results suggest that unmodified C_{60} and/or C_{60} metabolites by metabolic enzymes could be excreted into feces and/or urine. In further studies, the metabolic and excretion pathways of C_{60} should be evaluated to understand the toxicokinetics of C_{60}.

1. Introduction

Recent progress in the field of nanotechnology has resulted in the development of various newly engineered nanomaterials. Engineered nanomaterials are commonly produced in a wide variety of types, including fullerenes (C_{60}), carbon nanotubes (CNT), metal and metal oxide particles, polymer nanoparticles, and quantum dots. These materials have been applied to various fields of science and technology, and have increasingly been used for commercial purposes, such as fillers, opacifiers, catalysts, semiconductors, and personal care products (cosmetics and drugs) (Nel et al., 2006). On the other hand, there is insufficient information about the human health and environmental impact of nanomaterials, and concern about exposure to nanomaterials and the hazard that they pose is rising (Colvin, 2003; Moore, 2006).

Fullerene, a carbon nanomaterial, is a third allotropic form of carbon (after graphite and diamond). Unlike other carbon structures, fullerene is a closed cage carbon molecule with a truncated icosahedron structure that resembles a soccer ball with 12 pentagons and 20 hexagons (Kroto et al., 1985). Because of their unique structures and properties, fullerenes and their derivatives (endohedral fullerenes and chemically modified fullerenes) exhibit widely differing activities and therefore have attracted considerable attention. Since the water solubility of unmodified C_{60} is low, several studies have been performed to increase its water solubility by surface chemical modification and the formation of complexes with water soluble molecules (Bosi et al., 2003; Nakamura and Isobe, 2003), and as a result of these studies, a number of biological applications, such as free radical scavengers (Dugan et al., 1997), photoinduced DNA cleavage agents (Tokuyama et al., 1993), inhibitors of HIV-1 protease (Friedman et al., 1993), and cytotoxic agents to human cells (HDF, HepG2, and NHA) by lipid peroxidation (Sayes et al., 2005), for fullerene derivatives have been discovered. Rapid commercialization of fullerenes and their derivatives has increased the risk of occupational and environmental human exposure to these nanomaterials via oral, dermal, and inhalation uptake. However, little is known about the potential impact induced by exposure to nanomaterials (fullerenes and their derivatives) to human health, and comprehensive studies on the toxicology and biodistribution of fullerenes and their derivatives have been insufficient. To accurately evaluate the toxic effects of fullerenes and their derivatives by *in vivo* and *in vitro* assays, it is necessary to use an analytical chemical approach coupled with a biological approach. Several methods for analyzing fullerenes and their derivatives have been reported. However, only a few studies have

* Corresponding author. Tel.: +81 3 3700 9346; fax: +81 3 3700 9346.
E-mail address: reijik@nihs.go.jp (R. Kubota).

0378-4274/$ – see front matter © 2011 Elsevier Ireland Ltd. All rights reserved.
doi:10.1016/j.toxlet.2011.07.010

examined fullerenes and their derivatives in biological samples (Moussa et al., 1997; Xia et al., 2006), and the sensitivity of detection was insufficient and there was interference from the biological matrix in the analysis of samples. Several studies have investigated the biodistribution of fullerenes in rodents (Yamago et al., 1995; Cagle et al., 1999). However, the fullerenes used in these studies were water-soluble fullerene derivatives, and physical properties of these derivatives differ significantly from unmodified fullerene, especially water solubility; thus, it would be expected that the biodistribution characteristics of modified fullerene derivatives would also differ from unmodified fullerene. Furthermore, there are very few reports on the biodistribution of unmodified fullerene (including radiolabeled fullerene, such as ^{14}C-labeled C_{60} where the label is part of the C_{60} cage) (Bullard-Dillard et al., 1996) in rodents. In this study, we describe the biodistribution of unmodified C_{60} in rats after tail vein administration using a sensitive liquid chromatography–tandem mass spectrometry (LC–MS/MS) analytical method and liposomes as a carrier of unmodified C_{60}. Liposomes are known as one of the most effective drugs carrier. Moreover, the time-dependent biodistribution variation of unmodified C_{60} in rats was investigated, and the behavior of C_{60} after accumulated in tissues is discussed.

2. Methods

2.1. Chemicals and reagents

C_{60} (nanom purple SUH; purity >99.9%) was obtained from Frontier Carbon Corporation (Tokyo, Japan). C_{70} with a purity of 99.5% was purchased from Materials Technologies Research (Cleveland, USA). C_{70} was used for recovery correction of C_{60} extraction. HPLC grade acetonitrile and toluene were purchased from Wako Pure Chemical Industries, Ltd. (Osaka, Japan). Analytical grade acetic acid, disodium hydrogen phosphate, potassium chloride, potassium dihydrogen phosphate, sodium chloride, sodium dodecylsulfate, and chloroform were also purchased from Wako Pure Chemical Industries, Ltd. (Osaka, Japan). L-α-Phosphatidyl-choline and 3-sn-phosphatidyl-L-serine were purchased from Sigma–Aldrich (St. Louis, USA). Stock standard solutions were prepared by dissolving C_{60} (10 mg) and C_{70} (10 mg) in toluene (10 mL) with sonication and agitation and were stored at −20 °C until use. Working standard solutions were diluted with toluene from stock standard solution for the LC–MS/MS analysis.

2.2. Instrumentation

LC–MS/MS analysis was performed using a Waters Alliance 2695 HPLC system (Waters, Milford, USA) interfaced to a Waters Micromass Quattro Micro API triple quadrupole mass spectrometer equipped with an atmospheric pressure chemical ionization (APCI) interface (Waters, Milford, USA). System control and data handling were carried out by Waters MassLynx version 4.0.

2.3. Chromatographic and mass spectrometric conditions

Analysis of C_{60} was conducted as described previously (Kubota et al., 2009). The chromatographic separation was performed in isocratic mode at a flow rate of 1 mL/min with a mobile phase of 70% toluene and 30% acetonitrile. Fullerenes were separated using a Develosil RPFULLERENE column (5 μm, 4.6 mm × 250 mm) (Nomura Chemical Co., Ltd., Seto, Japan) at 30 °C (column oven temperature). The autosampler was kept at 10 °C and the injection volume was 20 μL. The mass spectrometer was operated in the APCI negative ion mode with multiple reaction monitoring (MRM). The APCI corona current was 15 μA, and the temperatures of the source and APCI probe were set to 120 °C and 400 °C, respectively. The desolvation and the cone gas flow rates were adjusted to 600 L/h and 50 L/h, respectively. The inter-scan delay was set to 0.1 s, and the inter-channel delay was set to 0.05 s. The dwell time was 0.5 s. Quantitation was performed using MRM of the reaction transitions of m/z = Q1 720 → Q3 720 for C_{60} and m/z = Q1 840 → Q3 840 for C_{70} (used for recovery correction of C_{60} extraction) with a collision energy of 60 eV and a cone voltage of 120 V. Multiple reaction monitoring (MRM) chromatogram of a 200 μg/L standard mixture of C_{60} and C_{70} was shown in Fig. 1.

2.4. Experimental animals

20 male Wistar rats (Slc: Wistar (SPF)) were purchased from Japan SLC, Inc. (Shizuoka, Japan) at six weeks of age. The rats were kept under Specific Pathogen Free (SPF) conditions with a 12 h light–dark cycle at the animal facility of the National Institute of Health Sciences (NIHS), Tokyo, Japan and were given tap water and autoclaved CRF-1 pellets (Oriental Yeast Co., Ltd., Tokyo, Japan) *ad libitum*. Experiments were humanely conducted under the regulation and permission of the Animal Care and Use Committee of NIHS.

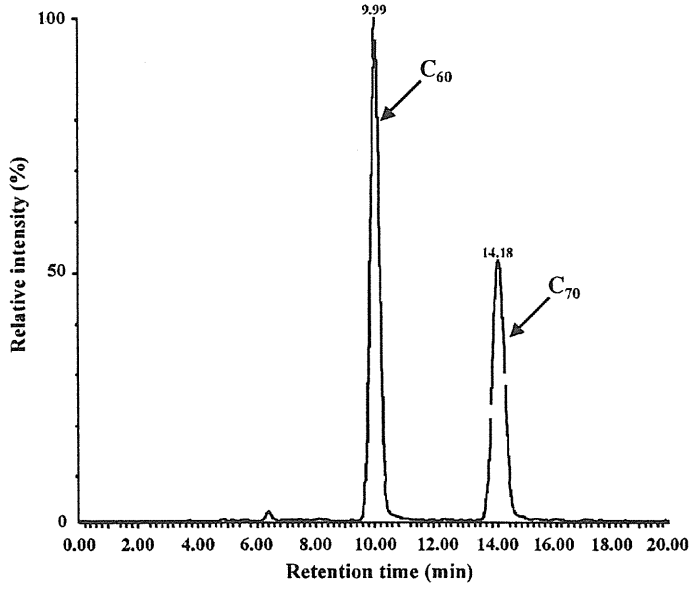

Fig. 1. Multiple reaction monitoring (MRM) chromatogram of a 200 μg/L mixture of C_{60} and C_{70}. Retention times (min) from top: C_{60} (9.99) and C_{70} (14.18).

2.5. Preparation of administration solution (C_{60}-liposome solution)

Because of the solubility of unmodified C_{60} is low, we used liposomes as a carrier of unmodified C_{60}. An administration solution for tail vein injection in rats was prepared as follows. L-α-Phosphatidyl-choline (PC) and 3-sn-phosphatidyl-L-serine (PS) were dissolved in chloroform as 25 mg/mL stock solutions and were stored at −80 °C until use. C_{60} was dissolved in toluene as a 2.5 mg/mL stock solution and was stored at 4 °C until use. A PC and PS mixture was prepared such that each component had a concentration of 0.5 mg/mL (PC:PS = 1:1 (w/w)) in chloroform. 1 mg/mL C_{60} solution (mixture of toluene and chloroform) was prepared by diluting the 2.5 mg/mL C_{60} stock solution with the lipid mixture and the mixture was gently volatilized with a stream of nitrogen gas. After volatilization, 1 × PBS buffer (pH 7.4), an amount equivalent to the mixture of toluene and chloroform, was added, and the mixture was vortexed for a few seconds. The liposomes containing C_{60} were sonicated using a bath sonicator for 10–15 min at 60 °C and were centrifuged at 1000 rpm for 10 s, and the supernatant (at room temperature) was used for tail vein administration. The supernatant was given to rats immediately and the solution was sonicated using a bath sonicator before each treatment to rats.

2.6. Treatment of experimental animals and sample collection

20 male Wistar rats at six weeks of age (five per group) were given repeated tail vein injections of 5 mL/kg body weight (one injection). A total of four tail vein injections (once per day) were performed (total injected C_{60}: ca. 929.1 μg). Rats were sacrificed on days 1, 7, 14, and 28 after completion of the injections. Brain, kidneys, liver, lungs, and spleen were collected from each rat and were rinsed with 1 × PBS buffer (pH 7.4). Moreover, blood (taken from the heart) was collected from each rat group. The collected tissues and blood samples were stored at −80 °C until analyzed.

2.7. Sample preparation

Extraction of C_{60} from tissues and blood of rats was performed according to the method of Kubota et al. (2009) with modifications. Freshly harvested whole tissues were weighted and placed in polypropylene copolymer (PPCO) centrifuge tubes. Tissues were frozen at −80 °C, and frozen tissues were freeze-dried over night. Each freeze-dried tissue was weighted and completely homogenized. In the case of small tissues (<0.5 g dry wt., brain, kidneys, spleen, and lungs), 0.2 M SDS solution (1 mL) and acetic acid (1 mL) were added to the centrifuge tubes, and the centrifuge tubes were vortexed and sonicated using a bath sonicator. An internal standard solution (C_{70} toluene solution, 0.5 mL) and 3.5 mL toluene were added to the centrifuge tubes, and they were shaken for 5 h at room temperature in the dark. After shaking, the centrifuge tubes were centrifuged for 30 min at 3500 rpm. 1 mL of supernatant was removed and placed in glass vials to be used for analysis. In the case of blood samples, untreated whole blood (2 mL, taken from the heart) was used for the extraction. Because the dry tissue weight of the liver (ca. 3 g dry wt.) was heavier than other tissues, a six-fold amount of each solution was used for the liver extraction. The limit of quantification (LOQ) in analytical solution was determined by analyzing

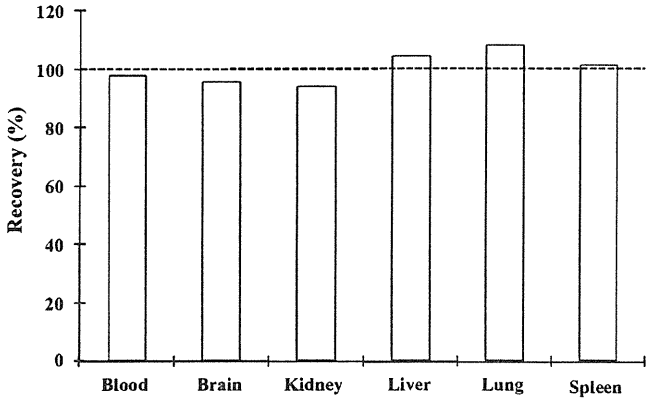

Fig. 2. Recovery of C_{60} from tissues and blood of rat.

the lowest level standard at least 5 times. The LOQ was calculated as 10-fold the standard deviation of these determinations. The LOQ value in analytical solution was 10 μg/L. Moreover, LOQ in each tissue was calculated by LOQ value in analytical solution, volume of toluene used for extraction, and tissue weight of each tissue. The LOQ for each tissue was 0.026 μg/g wet wt. for liver, 0.026 μg/g wet wt. for kidneys, 0.09 μg/g wet wt. for spleen, 0.046 μg/g wet wt. for lungs, and 0.023 μg/g wet wt. for brain, respectively.

2.8. Statistical analyses

Statistical analyses were performed using the program Excel Statistics (Ekuseru-Toukei 2008) (Social Survey Research Information Co., Ltd., Tokyo, Japan). Kolmogorov–Smirnov's test showed that some variables were not normally distributed. Therefore, non-parametric test was used for statistical analysis. Kruskal–Wallis test was used for validation of difference in the C_{60} concentrations in four tissues among treated groups. Where appropriate, Mann–Whitney's *U*-test, Scheffe's test, or Student's *t*-test was conducted to verify the difference in the C_{60} concentration in four tissues among each treated group.

3. Results

3.1. Recovery of C_{60} from tissues and blood of rat

A spike recovery test was conducted to evaluate the validity of the analytical method for determination of C_{60} in the tissues and blood of rat (Fig. 2). The recovery of C_{60} was determined by spiking samples collected from untreated rat. No C_{60} was observed in tissues and blood of untreated rat. 8 μL of C_{60} toluene solution (10 mg/L) was added to previously treated (tissues were freeze-dried, homogenized, added 0.2 M SDS and acetic acid, vortexed and sonicated.) tissues and blood (whole blood) giving a 20 μg/L final concentration, and was mixed. Thereafter, internal standard solution (toluene) and toluene were added and subsequent processes were conducted as described in Section 2. The recovery percentage was calculated by comparing the sample peak areas with those of the C_{60} standard solution at the same concentration (final concentration: 20 μg/L). Recovery percentages of C_{60} were 98.1% for blood, 95.7% for brain, 94.0% for kidneys, 105.0% for liver, 108.3% for lungs, and 101.4% for spleen, respectively. In the case of all tissues and blood as well as the internal standard, good recoveries were obtained. These results suggested that our method was valid for determining C_{60} concentrations in biological samples.

3.2. C_{60} concentrations in five tissues and blood of rats

C_{60} concentrations in tissues and blood of rats after tail vein injection were determined. Although no C_{60} was detected in the blood, C_{60} was observed in almost all of the tissues examined in this study (Table 1). For the Day 1 and Day 7 groups, C_{60} was detected in all samples from the five collected tissues of rats. C_{60} concentrations (mean ± SD) in tissues of the Day 1 rat group were 254 ± 114 μg/g wet wt. for lungs, 53.0 ± 18.8 μg/g wet wt. for spleen, 25.5 ± 5.56 μg/g wet wt. for liver, 1.30 ± 0.68 μg/g wet wt. for kidneys, and 0.08 ± 0.01 μg/g wet wt. for brain. C_{60} concentrations (mean ± SD) in tissues of the Day 7 rat group were 199 ± 88.4 μg/g wet wt. for lungs, 45.3 ± 10.7 μg/g wet wt. for spleen, 22.6 ± 9.63 μg/g wet wt. for liver, 0.42 ± 0.11 μg/g wet wt. for kidneys, and 0.04 ± 0.01 μg/g wet wt. for brain. For the Day 14 and Day 28 groups, although C_{60} was detected in all samples of the lungs, spleen, liver, and kidneys, C_{60} was only detected in one specimen of the Day 14 group in brain tissue. C_{60} concentrations (mean ± SD) in tissues of the Day 14 rat group were 109 ± 51.5 μg/g wet wt. for lungs, 59.0 ± 14.4 μg/g wet wt. for spleen, 21.9 ± 4.94 μg/g wet wt. for liver, 0.20 ± 0.02 μg/g wet wt. for kidneys, and 0.04 μg/g wet wt. (n = 1) for brain. C_{60} concentrations (mean ± SD) in tissues of the Day 28 rat group were 133 ± 47.5 μg/g wet wt. for lungs, 70.6 ± 32.0 μg/g wet wt. for spleen, 14.8 ± 3.00 μg/g wet wt. for liver, and 0.16 ± 0.04 μg/g wet wt. for kidneys.

Table 1
Concentrations of C_{60} in five tissues and blood of Wistar rats.

Group	Sample no.	Concentrations (μg/g wet wt.)					
		Lungs	Spleen	Liver	Kidneys	Brain	Blood
Day 1	1	223	46.5	19.9	1.10	0.080	<0.020
	2	207	78.6	20.8	0.807	0.074	<0.020
	3	188	34.8	32.4	1.14	0.062	<0.020
	4	456	38.7	30.2	0.954	0.078	<0.020
	5	197	66.4	24.5	2.49	0.096	<0.020
Day 7	6	152	52.1	23.0	0.542	0.029	<0.020
	7	281	56.8	18.8	0.508	0.034	<0.020
	8	235	45.0	39.1	0.431	0.048	<0.020
	9	259	28.7	15.4	0.292	0.032	<0.020
	10	66.9	43.8	16.9	0.327	0.037	<0.020
Day 14	11	105	68.3	17.8	0.200	<0.023	<0.020
	12	74.0	51.0	27.9	0.235	<0.023	<0.020
	13	67.5	62.1	17.9	0.200	0.035	<0.020
	14	103	75.1	19.3	0.168	<0.023	<0.020
	15	196	38.8	26.7	0.189	<0.023	<0.020
Day 28	16	113	110	11.4	0.129	<0.023	<0.020
	17	204	94.9	16.6	0.111	<0.023	<0.020
	18	142	68.2	18.3	0.156	<0.023	<0.020
	19	133	44.4	12.0	0.191	<0.023	<0.020
	20	74.1	35.1	15.8	0.191	<0.023	<0.020

4. Discussion

4.1. Biodistribution of C_{60} in rats

C_{60} concentrations in tissues and blood of rats after tail vein injection are investigated (Table 1). C_{60} was detected in the lungs, spleen, liver, and kidneys of rats in all groups, ranging from 0.16 ± 0.04 μg/g wet wt. (kidneys, Day 28) to 254 ± 114 μg/g wet wt. (lungs, Day 1). The highest C_{60} concentration was detected in the lungs, followed by spleen, liver, and kidneys. On the other hand, although C_{60} was detected in all of the brains from the Day 1 and Day 7 groups (0.08 ± 0.01 μg/g wet wt. for Day 1; 0.04 ± 0.01 μg/g wet wt. for Day 7), C_{60} was detected in only one brain specimen from the Day14 group (0.04 μg/g wet wt.) and none of the specimens from the Day 28 group. Moreover, no C_{60} was observed in blood samples from any of the groups. Although studies of the biodistribution of unmodified C_{60} are limited, several studies have reported the biodistribution of water-soluble C_{60} derivatives. Yamago et al. (1995) reported the biodistribution of ^{14}C-labeled water-soluble C_{60} in Fischer rats after intravenous injection. After injection, ^{14}C-labeled water-soluble C_{60} was rapidly removed from blood and about 80% of ^{14}C-labeled water-soluble C_{60} was retained

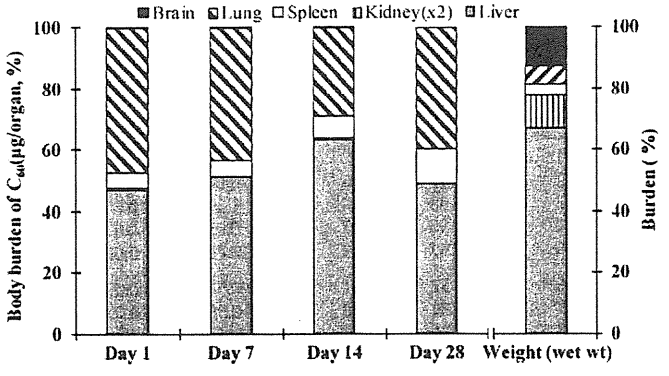

Fig. 3. Comparison of C_{60} distribution in tissues of the four treated rat groups (Days 1, 7, 14, and 28).

in the liver until after 30 h. Furthermore, ^{14}C-labeled water-soluble C_{60} was also detected as a minor component in the spleen, lungs, kidneys, heart, testicles, and brain (Yamago et al., 1995). Bullard-Dillard et al. (1996) reported that a ^{14}C-labeled C_{60} where the label is part of the C_{60} cage after injection in Sprague–Dawley rats was rapidly cleared from the circulation with the majority of the radiolabel accumulated in the liver (90–95%) and ^{14}C-labeled C_{60} was not eliminated from the liver over the 120 h. Moreover, ^{14}C-labeled water-soluble C_{60} derivative was found in liver (>50%) with another 28% distributed between muscle, skin, and lung (Bullard-Dillard et al., 1996). Nikolić et al. (2009) indicated that significantly higher accumulation of radiolabeled C_{60} (^{125}I-nanoC_{60}) was observed in liver as well as spleen, while the accumulation of radiolabeled C_{60} was lower in the lungs, intestines and bone of Wistar rats after intravenous injection. Furthermore, Cagle et al. (1999) showed the selective localization of water-soluble radioactive metallofullerene in the liver of BALB/c mice after intravenous administration. In contrast, although C_{60} was found in the lungs, spleen, liver, kidneys, and brain, in our study the highest concentration of C_{60} was observed in the lungs and the trend differed from the other studies (Yamago et al., 1995; Bullard-Dillard et al., 1996; Cagle et al., 1999; Nikolić et al., 2009). In this study, C_{60}-liposome was suspended in the administration solution, and the C_{60} was an unmodified form. Hence, the difference in the biodistribution of C_{60} between previous studies and this study might be attributable to differences in physical properties, the particle size distribution of C_{60} in the administration solution, and/or period after completion of the injections. Compared with previous studies, the C_{60} particle size in the administration solution for this study seems large (particle size: >100 nm, particle size was obtained from measuring of diluted administration solution by Zetasizer Nano, Malvern Instruments Ltd.) because the C_{60} water solubility is low. We considered that C_{60} injected in the tail vein could be filtered by lung capillary vessels and accumulate in the lungs prior to being distributed to other tissues. C_{60} not being detected in the blood indicates that clearance of C_{60} from the blood by filtration might effectively occur in the lungs. Although C_{60} concentrations were low (0.029–0.096 μg/g wet wt.), C_{60} was detected in the brain. Yamago et al. (1995) and Cagle et al. (1999) have also reported that C_{60} was observed in the brain at low concentrations. These results suggest that a low concentration of C_{60} can pass through the blood brain barrier and accumulate in the brain.

The distribution of C_{60} burden among the five rat tissues was calculated from the product of the C_{60} concentration in each tissue and the weight of each tissue (Fig. 3). Among five tissues, the C_{60} burden was highest in the liver (47.3–63.6%), followed by the lungs (29.0–47.5%), spleen (4.9–11.1%), kidneys (0.1–0.4%), and brain (0–0.03%). Although C_{60} concentrations in the liver were lower than those in the lungs and spleen, the liver showed a higher percentage of C_{60} burden (47.3–63.6%) as a result of the large liver mass (67.0%). On the other hand, although the spleen and lungs accounted for 3.2% and 6.2% of the mass of the five tissues, respectively, the C_{60} burdens were 4.9–11.1% for the spleen and 29.0–47.5% for the lungs, respectively. These three tissues accounted for approximately 100% of the C_{60} burden, indicating that C_{60} was localized to the lungs, spleen, and liver. Because capillary vessels are abundant in these tissues, C_{60} might accumulate by filtration in these tissues. In this study, we focused on the lungs, spleen, liver, kidneys, and brain as major target organs, and other tissues, urine and feces of each specimen were not collected. Although several studies reported the detection of C_{60} derivatives in other tissues (such as, bone, fat, heart, intestines, muscle, and testicles), C_{60} derivatives in these tissues were mostly observed as minor components (Yamago et al., 1995; Bullard-Dillard et al., 1996; Cagle et al., 1999; Nikolić et al., 2009). Further studies should evaluate the metabolic and excretion pathways of C_{60} in experimental animals to understand the toxicokinetics of C_{60}.

4.2. Time-dependent variation in the biodistribution of C_{60} in rats

The time-dependent variation in the biodistribution of C_{60} in rats was examined by comparison of C_{60} concentrations in the five tissues from the four rat groups (Days 1, 7, 14, and 28) (Fig. 4). Although the number of samples for each group was small ($n = 5$), a time-dependent decrease in C_{60} concentrations was observed in all tissues, except the spleen. A significant decrease in C_{60} concentration was found in the kidneys and brain. In the case of the kidneys, significant difference in C_{60} concentration from the four treated groups was found (Kruskal–Wallis test, $p = 0.0007$). C_{60} concentrations from the Day 14 group were significantly lower than those from the Day 1 group (Scheffe's test, $p = 0.0396$). Moreover, C_{60} concentrations from the Day 28 group were also significantly lower than those of the Day 1 group (Scheffe's test, $p = 0.0024$). In the case of the brain, C_{60} concentrations from the Day 7 group were significantly lower than those from the Day 1 group (Student's t-test, $p = 0.0002$). Furthermore, C_{60} concentrations of the Day 14 and Day 28 groups were also lower than those of the Day 7 group. On the other hand, in the lungs and liver, the decreasing trend in C_{60} concentration was slower as compared with the trend in the kidneys and brain. In the case of the lungs, significant difference in C_{60} concentration from the four treated groups was found (Kruskal–Wallis test, $p = 0.0493$) and C_{60} concentrations from the Day 14 group were significantly lower than those from the Day 1 group (Mann–Whitney's U-test, $p = 0.0163$). In the case of the liver, significant difference in C_{60} concentration from the four treated groups was found (Kruskal–Wallis test, $p = 0.0251$) and C_{60} concentrations from the Day 28 group were significantly lower than those from the Day 1 group (Scheffe's test, $p = 0.0298$).

Although with shorter experimental periods than this study, several studies have reported a time-dependent variation in the concentration of C_{60} derivatives in tissues. Yamago et al. (1995) reported the time-dependent change in tissue radioactivity levels using ^{14}C-labeled water-soluble C_{60}. In the liver, about 80% of the total radioactivity was retained after 30 h, and was mostly eliminated (1.6%) after 160 h. This decrease in radioactivity was also observed in the spleen, lungs, and brain. Cagle et al. (1999) also reported the time-dependent decrease of water-soluble radioactive metallofullerene in liver, kidneys, lungs, spleen, and brain after 48 h. Although these studies found a time-dependent decrease of C_{60} derivatives in various tissues, differences in the decreasing trend of the C_{60} derivatives among tissues were not observed. In our study, different decreasing trends of C_{60} among tissues were observed. In the kidneys and brain, a significant decrease in C_{60} concentration was observed. On the other hand, C_{60} concentration

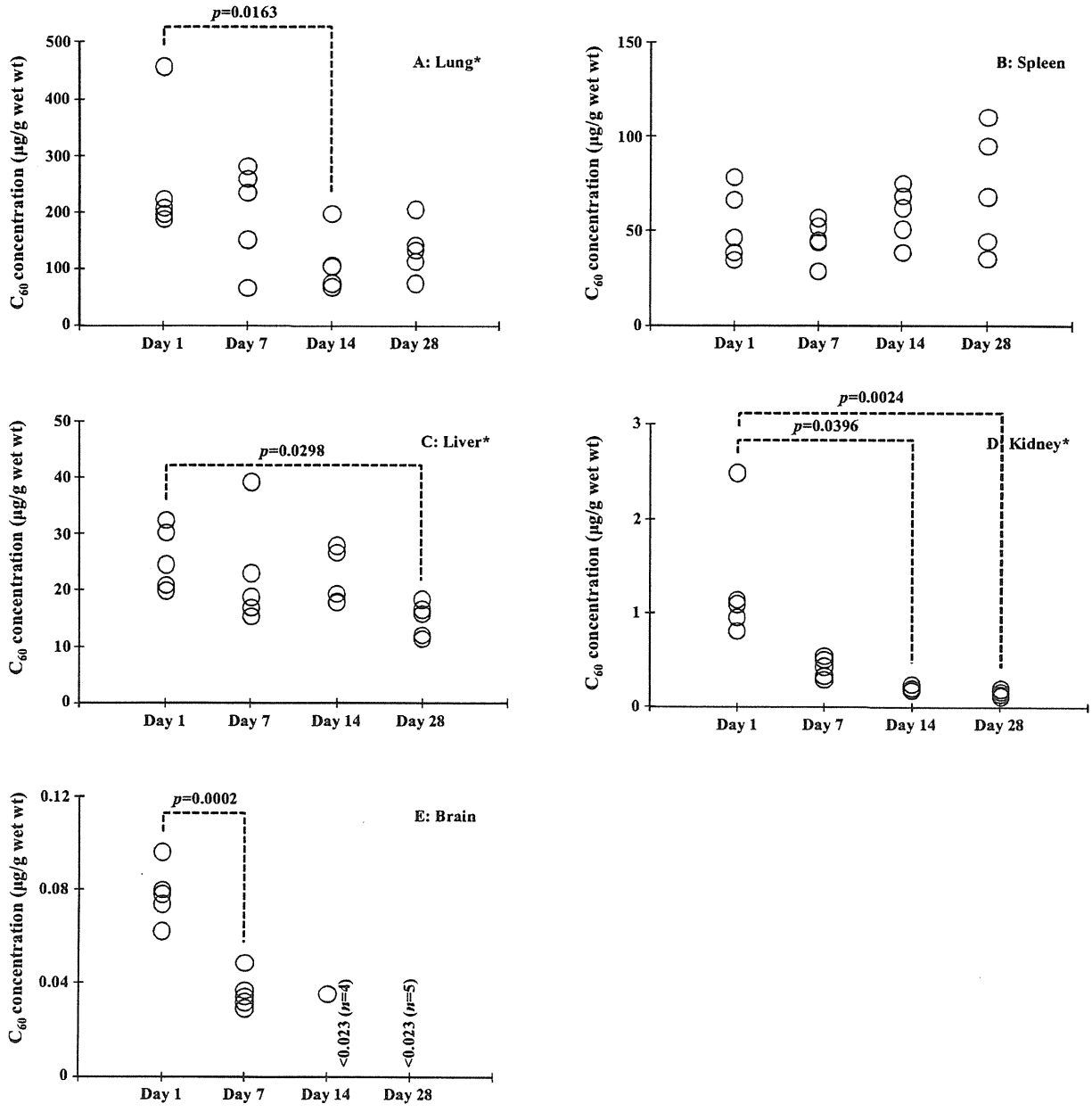

Fig. 4. Comparison of C_{60} concentrations in each tissue of the four treated rat groups (Days 1, 7, 14, and 28). Kruskal–Wallis test was used for validation of difference in the C_{60} concentrations in four tissues among treated groups and significant difference (*) was observed in lungs ($p = 0.0493$), liver ($p = 0.0251$), and kidneys ($p = 0.0007$). (A) C_{60} concentration in lungs (Day 14 vs. Day 1, $p = 0.0163$ (Mann–Whitney's *U*-test)). (B) C_{60} concentration in spleen. (C) C_{60} concentration in liver (Day 28 vs. Day 1, $p = 0.0298$ (Scheffe's test)). (D) C_{60} concentration in kidneys (Day 14 vs. Day 1, $p = 0.0396$ (Scheffe's test); Day 28 vs. Day 1, $p = 0.0024$ (Scheffe's test)). (E) C_{60} concentration in brain (Day 7 vs. Day 1, $p = 0.0002$ (Student's *t*-test)).

in lungs and liver decreased gradually. This difference of decreasing trends among tissues could be due to differences in accumulation levels. The low concentration of C_{60} in the kidneys and brain might be easily decreased compared to the high concentrations of C_{60} in the lungs, liver, and spleen. Although it is not clear whether C_{60} is excreted from the body, we propose some possible mechanisms for the decrease of C_{60} in tissues. The first possible mechanism is redistribution to other tissues via blood. Although only five tissues were examined in this study, C_{60} might be detectable in other organs. Cagle et al. (1999) reported a comparatively high concentration of water-soluble radioactive metallofullerene in bone. Moreover, although the accumulation levels were low, radiolabeled nano C_{60} (^{125}I-nanoC_{60}) was found in intestines and bone of rats (Nikolić et al., 2009). Although the C_{60} concentration in blood was below the limit of detection, the small blood volume used for the analysis could be the reason for this result. If a larger volume of blood were analyzed, C_{60} might be detected. Bullard-Dillard et al. (1996) reported that 0.39% of ^{14}C-labeled C_{60} was detected in blood of rat at 120 h post-injection. The second possible mechanism is metabolism to water-soluble fullerene metabolites and excretion into urine. Although there is no information on the intravital metabolism of C_{60}, it is possible that C_{60} could be metabolized to C_{60} derivatives (e.g. fullerenol ($C_{60}(OH)_n$)) by metabolic enzymes (e.g. cytochrome P450). Hamano et al. (1995) identified the structures of $C_{60}O$, $C_{60}O_2$, and $C_{60}O_3$ formed in P450 chemical model systems and the results support the hypothesis that possibility of a biotransformation of C_{60} into more hydrophilic C_{60} derivative capable of being excreted into the urine. In this study, the renal C_{60} concentration rapidly decreased, which also supports the possibility that C_{60} is excreted from urine. The third possible mechanism is biliary

excretion of unmodified C_{60} and/or C_{60} metabolites. Because C_{60} is lipophilic, if C_{60} is excreted without metabolism, it might be via this route. Consequently, further studies are required to verify the metabolism and excretion of C_{60}. Yamago et al. (1995) reported that virtually all of the excretion of ^{14}C-labeled water-soluble C_{60} occurred via the feces and 5.4% of ^{14}C-labeled water-soluble C_{60} was eliminated into the feces after 160 h in intravenous injection experiment. Moreover, Cagle et al. (1999) also indicated that a water-soluble radioactive metallofullerene was excreted into the feces of rats.

In summary, the current study demonstrates that C_{60} after tail vein administration is widely distributed between various tissues, such as brain, kidneys, liver, lungs, and spleen of rats. Moreover, the large variability in C_{60} concentrations among tissues was found and the highest C_{60} concentration was observed in the lungs, followed by spleen, liver, kidneys, and brain. These results suggested that C_{60} injected in the tail vein could be filtered by lung capillary vessels and accumulate in the lungs prior to being distributed to other tissues. Furthermore, C_{60} not being detected in the blood indicates that clearance of C_{60} from the blood by filtration might effectively occur in the lungs. A time-dependent decrease in C_{60} concentrations was observed in all tissues, except spleen. Moreover, a decreasing trend of C_{60} levels differed among tissues, which could be due to differences in accumulation. These results suggest that unmodified C_{60} and/or C_{60} metabolites by metabolic enzymes could be excreted into feces and/or urine. In further studies, the metabolic and excretion pathways of C_{60} should be evaluated to understand the toxicokinetics of C_{60}.

Conflict of interest

The authors declare that there are no conflicts of interest.

Acknowledgement

We are grateful to Miss Rika Maekawa and Mr. Masaki Tsuji for technical support. This study was supported by H21-kagaku-ippan-008 from the Ministry of Health, Labour and Welfare, Japan.

References

Bosi, S., Da Ros, T., Spalluto, G., Prato, M., 2003. Fullerene derivatives: an attractive tool for biological applications. Eur. J. Med. Chem. 38 (11–12), 913–923.
Bullard-Dillard, R., Creek, K.E., Scrivens, W.A., Tour, J.M., 1996. Tissue sites of uptake of ^{14}C labeled C_{60}. Bioorg. Chem. 24 (4), 376–385.
Cagle, D.W., Kennel, S.J., Mirzadeh, S., Alford, J.M., Wilson, L.J., 1999. In vivo studies of fullerene-based materials using endohedral metallofullerene radiotracers. Proc. Natl. Acad. Sci. U.S.A. 96, 5182–5187.
Colvin, V.L., 2003. The potential environmental impact of engineered nanomaterials. Nat. Biotechnol. 21 (10), 1166–1170.
Dugan, L.L., Turetsky, D.M., Du, C., Lobner, D., Wheeler, M., Almli, C.R., Shen, C.K.F., Luh, T.Y., Choi, D.W., Lin, T.S., 1997. Carboxyfullerenes as neuroprotective agents. Proc. Natl. Acad. Sci. U.S.A. 94, 9434–9439.
Friedman, S.H., DeCamp, D.L., Sijbesma, R.P., Srdanov, G., Wudl, F., Kenyon, G.L., 1993. Inhibition of the HIV-1 protease by fullerene derivatives: model building studies and experimental verification. J. Am. Chem. Soc. 115, 6506–6509.
Hamano, T., Mashino, T., Hirobe, M., 1995. Oxidation of [60]fullerene by cytochrome P450 chemical models. J. Chem. Soc. Chem. Commun. 15, 1537–1538.
Kroto, H.W., Heath, J.R., O'Brien, S.C., Curl, R.F., Samlley, R.E., 1985. Nature 318 (14), 162–163.
Kubota, R., Tahara, M., Shimizu, K., Sugimoto, N., Hirose, A., Nishimura, T., 2009. Development of a liquid chromatography–tandem mass spectrometry method for the determination of fullerenes C_{60} and C70 in biological samples. Bull. Natl. Inst. Health Sci. 127, 65–68.
Moore, M.N., 2006. Do nanoparticles present ecotoxicological risks for the health of the aquatic environment? Environ. Int. 32, 967–976.
Moussa, F., Pressac, M., Genin, E., Roux, S., Trivin, F., Rassat, A., Célin, R., Szwarc, H., 1997. Quantitative analysis of C_{60} fullerene in blood and tissues by high-performance liquid chromatography with photodiode-array and mass spectrometric detection. J. Chromatogr. B 696, 153–159.
Nakamura, E., Isobe, H., 2003. Functionalized fullerenes in water. 2003. The first 10 years of their chemistry, biology, and nanoscience. Acc. Chem. Res. 36 (11), 807–815.
Nikolić, N., Vranjes-Ethurić, S., Janković, D., Ethokić, D., Mirković, M., Bibić, N., Trajković, V., 2009. Preparation and biodistribution of radiolabeled fullerene C_{60} nanocrystals. Nanotechnology 20, 385102.
Nel, A., Xia, T., Mädler, L., Li, N., 2006. Toxic potential of materials at the nanolevel. Science 3, 622–627.
Sayes, C.M., Gobin, A.M., Ausman, K.D., Mendez, J., West, J.L., Colvin, V.L., 2005. Nano-C_{60} cytotoxicity is due to lipid peroxidation. Biomaterials 26, 7587–7595.
Tokuyama, H., Yamago, S., Nakamura, E., 1993. Photoinduced biochemical activity of fullerene carboxylic acid. J. Am. Chem. Soc. 115, 7918–7919.
Xia, X.R., Monteiro-Riviere, N.A., Riviere, J.E., 2006. Trace analysis of fullerenes in biological samples by simplified liquid–liquid extraction and high-performance liquid chromatography. J. Chromatogr. A 1129, 216–222.
Yamago, S., Tokuyama, H., Nakamura, E., Kikuchi, K., Kananishi, S., Sueki, K., Nakahara, H., Enomoto, S., Ambe, F., 1995. In vivo biological behavior of a water-miscible fullerene: ^{14}C labeling, absorption, distribution, excretion and acute toxicity. Chem. Biol. 2, 385–389.

—Review—

ナノマテリアルの慢性影響研究の重要性

広瀬明彦,*,[a] 高木篤也,[a] 西村哲治,[a] 津田洋幸,[b] 坂本義光,[c]
小縣昭夫,[c] 中江　大,[c] 樋野興夫,[d] 菅野　純[a]

Importance of Researches on Chronic Effects by Manufactured Nanomaterials

Akihiko HIROSE,*,[a] Atsuya TAKAGI,[a] Tetsuji NISHIMURA,[a]
Hiroyuki TSUDA,[b] Yoshimitsu SAKAMOTO,[c] Akio OGATA,[c]
Dai NAKAE,[c] Okio HINO,[d] and Jun KANNO[a]

[a]Division of Risk Assessment, National Institute of Health Sciences, Kamiyoga 1–18–1, Setagaya-ku, Tokyo 158–8501, Japan, [b]Nagoya City of University, 1 Kawasumi Mizuho-cho, Mizuho-ku, Nagoya 467–8601, Japan, [c]Tokyo Metropolitan Institute of Public Health, 3–24–1 Hyakunin-cho, Shinjyuku-ku, Tokyo 169–0073, Japan, and [d]Juntendo University School of Medicine, 2–1–1 Hongo, Bunkyo-ku, Tokyo 113–8421, Japan

(Received September 3, 2010)

Manufactured nanomaterials are the most important substances for the nanotechnology. The nanomaterials possess different physico-chemical properties from bulk materials. The new properties may lead to biologically beneficial effects and/or adverse effects. However, there are no standardized evaluation methods at present. Some domestic research projects and international OECD programs are ongoing, in order to share the health impact information of nanomaterails or to standardize the evaluation methods. From 2005, our institutes have been conducting the research on the establishment of health risk assessment methodology of manufactured nanomaterials. In the course of the research project, we revealed that the nanomaterials were competent to cause chronic effects, by analyzing the intraperitoneal administration studies and carcinogenic promotion studies. These studies suggested that even aggregated nanomaterials were crumbled into nano-sized particles inside the body during the long-term, and the particles were transferred to other organs. Also investigations of the toxicokinetic properties of nanomaterials after exposure are important to predict the chronically targeted tissues. The long lasting particles/fibers in the particular tissues may cause chronic adverse effects. Therefore, focusing on the toxicological characterization of chronic effects was considered to be most appropriate approach for establishing the risk assessment methods of nanomaterials.

Key words——chronic toxicity; multi-wall carbon nanotube (MWCNT); fullerene

1. はじめに

近年，ナノテクノロジーの中心的な役割を担う物質としての産業用ナノマテリアルは，急速にその種類や生産量が増加しつつあるところであるが，新たに期待されているナノマテリアルの物理化学特性については，有効的な生理活性等に使用され得る特性を持つ反面，ヒト健康影響に対する懸念についても検証されるべきであると考えられている．つまり，ナノマテリアルを用いた技術や製品を社会的に受容するためには，安全性の検証を行うことが不可欠であると思われる．しかし，従来の一般的な化学物質とは異なる物理化学的特性は，その毒性評価においても従来とは異なる考え方を取り入れることも必要とされている．それゆえ，ナノマテリアルの特性を考慮した有害性評価手法の開発が急務となっている．また，国際的な枠組みにおいても，ナノマテリアルの安全性確認は，重要な問題として認識されており，OECD や ISO 等を中心として評価手法の国際的標準化に向けた取り組みが進行しているところでもある．本稿では，ナノマテリアルの安全性評価

[a]国立医薬品食品衛生研究所（〒158–8501 東京都世田谷区上用賀 1–18–1），[b]名古屋市立大学（〒467–8601 名古屋市瑞穂区瑞穂町字川澄 1），[c]東京都健康安全研究センター（〒169–0073 東京都新宿区百人町 3–24–1），[d]順天堂大学医学部（〒113–8421 東京都文京区本郷 2–1–1）
*e-mail: hirose@nihs.go.jp

本総説は，日本薬学会第 130 年会シンポジウム S18 で発表したものを中心に記述したものである．

の確立に向けたこれらの取り組みに貢献してきたわれわれの研究成果の一部と，それらの研究結果から帰納的に導き出された慢性影響評価研究の重要性について論ずる．

2. ナノマテリアルのリスク評価法の確立における課題

一般的に，化学物質の健康影響評価（リスクアセスメント）の基本的なフレームは，有害性評価と曝露評価，及び各々の評価内容を比較・統合化する過程のリスク判定のステップから成り立っている．この基本的なフレーム自体は，ナノマテリアルの健康影響評価に適用できるものであると考えられる．[1-5] しかし，ナノマテリアルに特徴的な新たな物理化学的性質，特にサイズが生体内高分子と近いことや，高い表面活性のために凝集し易い性質を考慮すると，よりサイズの大きい通常のバルク化合物や完全に溶解した単一分子化合物とは，生体内挙動が異なることが予想され，同じ化学組成の化合物であってもその毒性発現部位や発現様式は異なることが予想される．つまり，体内動態［吸収 absorption，分布 distribution，代謝 metabolism，排泄 excretion（ADME）］情報は，一般の化学物質より重要な意味を持つと考えられる．

そこで，生体内での挙動を把握するためには，生体試料中で検出，同定・定量できる方法を確立しなくてはならない．一般にナノマテリアルの開発段階において，その性質を把握するための物理化学的測定法も同時に開発されているはずであるが，それらの手法は生体試料中に存在するナノマテリアルにそのまま適用できないことも多い．さらに，機器分析法による生体試料中での検出や定量が可能になったとしても，生体内で実際にナノの状態で存在しているのか，あるいは再凝集などはしていないかなど，標的組織における最終的な生体内反応に影響を及ぼすと考えられる実際のナノマテリアルの存在状態を把握するためには，最終的には，組織標本の電子顕微鏡などによる確認が必要となる．

一方，体内動態に影響を与える因子として，投与法を検討する必要もある．単独では凝集し易いナノマテリアルをそのまま曝露するということは，物理的に巨大となった粒子は体への吸収性が低く，ナノマテリアル自体の体内動態や懸念される有害性を検出することが困難になると考えられるためである．そのために曝露実験時におけるナノマテリアルの分散手法の開発が必要となる．職業曝露などの比較的大量のナノマテリアル曝露の安全性を評価するという観点からは，凝集したままの曝露にも意義があるかもしれないが，製品中への混入や環境中への排出を経由した，分散された曝露も想定されることは考慮すべきであると考えられる．

Figure 1 は，凝集したナノマテリアルが，生体に取り込まれた場合に想定される体内動態を模式図化したものである．ナノマテリアルの使用用途にも依存するが，製品中のナノマテリアルはポリマー等の他の高分子化合物等と混合された状態，あるいはナノマテリアルだけが単独で製品から解離していく状態を考慮しても，この凝集性のために，大きな粒子として曝露する可能性が高いものと想定される．急性的には，このサイズの大きくなった物質は生体に取り込まれることはほとんどなく，局所的な刺激を起こすような変化を除いては，生体内で有害性が惹起される可能性は低いものと考えられる．しかし，仮に凝集したナノマテリアルが長期間に渡って，吸収部位である肺胞や消化管，損傷皮膚などの局所に滞留したり，慢性的に曝露したりするケースを想定すると，時間経過とともに小さくなった凝集体の粒子を除去するために，マクロファージなどの食細胞による取り込みや，表面活性の高いナノマテリアル分子と生体成分との結合作用による侵食作用により，生体に少しずつ取り込まれることが想定される．もしも生体内に取り込まれたナノマテリアルと生体内成分との結合性が高い場合には，容易に生体外に排出されることはなく，特定の組織等へ蓄積し易くなり，慢性影響の可能性を検討する必要が出てくると想定できる．

3. 国立医薬品食品衛生研究所における取り組みの成果の概要

以上のナノマテリアル固有の検討課題を考慮して，われわれは 2005 年より厚生労働科学研究の化学物質リスク研究事業の枠組みの中で，ナノマテリアルの健康影響評価手法の開発に係わる研究を推し進めてきたところである．われわれは，これらの検討課題を解決するために，Fig. 2 に示すように 4 つの項目を中心に研究を行ってきた．これらの項目の中で，*in vivo* 研究については，比較的研究初期の段階から中心的に取り組んできた．その中で，繊維

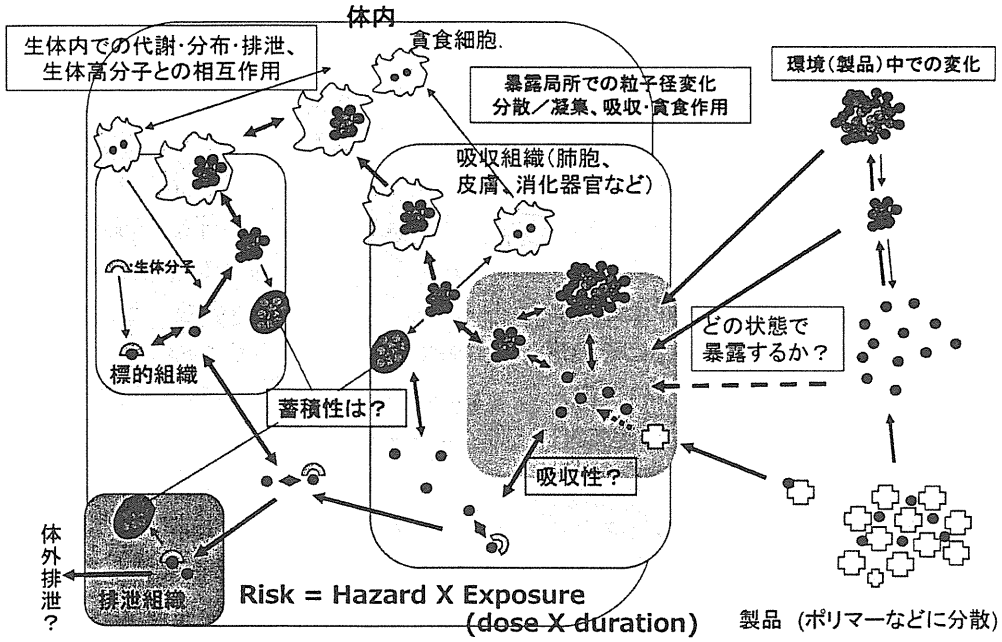

Fig. 1. The Estimated ADME Schema of Nanomaterials

***in vivo*試験法研究**

MWCNTのP53ヘテロ欠失マウスへのi.p.投与による中皮腫誘発性を確認
バイオマーカとしてマウスのメソセリン抗体の作成
一方、C60の腹腔内投与による慢性的影響として腎臓への影響を示唆
TiO_2と C60の気管内投与による発がんプロモーション作用の示唆

吸入試験法研究

MWCNTのミスト暴露システムを開発
気管内投与時の分散性依存の発現様式差異を確認
リポソーム分散C60による気管内投与法を開発。

暴露測定法／動態解析研究

生体試料でのC60の定量的検出法との確立
静注後のC60の組織からの経時的消失検討
気管内投与後のMWCNTの肺及び肝臓での検出

***in vitro*試験法研究**

細胞培養系でのリポソーム等を用いた分散法の確立
→C60やTiO_2の遺伝毒性、細胞透過性、
神経系の細胞機能への影響、などへの適用

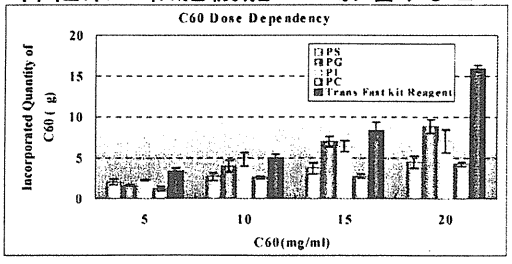

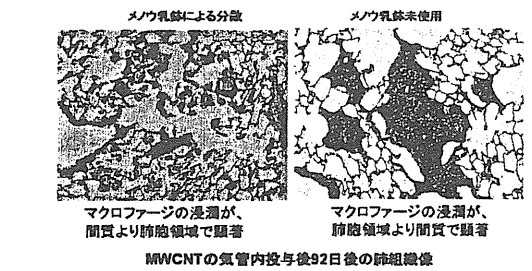

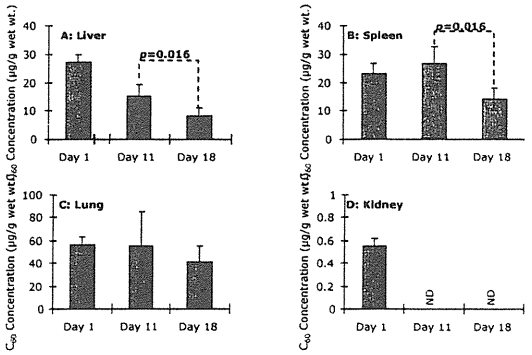

C_{60}のラットへの尾静脈投与（12.5 μg/kg）における体内分布
反復(4回)投与後の体内分布の経時変化

Fig. 2. The Overall Results of NIHS Projects for Nanomaterial Safety

長の長いタイプの多層型カーボンナノチューブ（MWCNT）が，中皮腫を誘発する可能性を持つことを確認した.[6] 上記の体内動態の重要性を考慮した概念からは，吸収性や体内分布について検証したのちに，慢性影響の可能性を検討することが論理的であるが，研究開始当時から，大量生産可能であった，酸化チタン（TiO_2）やフラーレン（C60），MWCNTについては，*in vivo*の慢性影響を先行して検討しておくべきであると判断した．特にその形状がアスベストに似ていたMWCNTについては，吸入曝露による有害影響が懸念されたが，MWCNTについての吸入曝露法が確立していない段階では，アスベストでも検証に使用されていた腹腔内投与による中皮腫誘発試験を行うこととした．

われわれの最初の実験は，アスベストで中皮腫の誘発時期が早くなることが知られているp53ヘテロノックアウトマウスへの腹腔内へ3 mg/mouseという高用量を投与することによって確認されたものであり，動物種の特異性や投与量の多さについて異論も指摘された．しかしその後の研究で，野生型の動物種であるF344ラットに対しても，同じMWCNTが中皮腫の誘発作用を持つことが確認された[7]ほか，投与量を1000分の1にまで少なくした実験においても中皮腫の起きることが示されている（投稿中）．

酸化チタンについては，雌ラットへの吸入曝露により発がん性のあることが示されているが，ナノサイズ化による発がん性の検証のために，気管内投与による肺がんのプロモーション作用の検討を行った．その結果，酸化チタンは，肺腺腫や乳腺腫に対してプロモーション作用を示し，その作用は，マクロファージから放出される炎症性因子であるMIP1αを介したものであることが示唆された.[8] 現在C60やMWCNTを用いたプロモーション作用の検討が進行中である．

一方，曝露手法の開発においては，ミスト法や粉体法によるMWCNTの吸入曝露システムの開発研究を進めているが，より簡易な手法として気管内投与のための適切な分散法の検討を行った．その結果，分散法の違いが肺の有害性発現様式に違いを引き起こすことを確認した.[9]

体内動態解析のために，生体試料中のC60やTiO_2の分析手法の開発や改良を行い，経口投与や気管内投与による体内吸収性について検討を行っている．現在のところ投与部位である消化管や肺以外で有意な検出量を確認できておらず，感度の向上に向けた研究を進めている．しかし，体内への吸収を前提にした解析として，C60の静脈内投与による解析を行ったところ，肝臓や脾臓，肺などへの分布を確認したが，腎臓への分布は極めて低いことが示された（投稿中）．その他，遺伝毒性や標的臓器などの毒性をスクリーニングするための*in vitro*試験における培地等への分散法も検討対象としており，リポソームを用いたC60の分散法を確立した．

4. 慢性影響研究の重要性

ナノマテリアルの生体影響に関する情報はここ数年の活発な研究状況を反映して多くなりつつあるが，慢性影響に関する報告は依然その数が少ない状況である．一般の化学物質の有害性評価の常套手段として，変異原性試験や短期試験から情報を収集していくことは，必要なステップであり，OECDにおけるナノマテリアル作業グループの活動におけるスポンサーシッププログラムにおいても，加盟各国からの毒性試験情報として，短期試験を中心に収集されてきている．われわれの研究グループにおいても，これらの枠組みに対して，短期的な試験情報を中心に提供し始めている段階である．しかしMWCNTに関しては，研究初期から，短期毒性より長期毒性の方が懸念の強いことが，物性等の情報から推測されたところでもあり，その推定に基づいて，腹腔内投与の研究を最初にスタートさせた．腹腔内投与は，リスク評価の観点からは，曝露経路（吸入曝露）に伴う定量的な評価に問題のあるところであるが，最近の注目すべき研究として，分散剤で分散させたMWCNT（最高80 μgまで）をマウスに吸引させた研究や，MWCNT: 30 mg/m^{3}をマウスに単回吸入曝露した研究において，曝露後7–8週間目にMWCNTが胸膜に到達していたことが報告されている.[10,11] これらの研究結果は高用量の曝露による短期間の結果ではあるが，呼吸器を経由した曝露においてもMWCNTは胸膜（中皮）まで到達することを示唆しており，われわれの腹腔内投与による結果と合わせると，リスク評価の上でも重要な知見であると考えられる．

これらの腹腔内投与による中皮腫誘発能は，繊維状粒子による催腫瘍性のみを検出する系であり，短

いタイプやその他様々な形状のMWCNTにおける慢性毒性は別途検証する必要性がある．実際，われわれの行った腹腔内投与試験では，小さいサイズのナノチューブ繊維を含んだ細胞が腹膜の病変部のみならず，肝類洞内，又は肝葉間や腸間膜リンパ節の中にも認められ，体内に再分布することが示唆された（Fig. 3）.[6] さらに，SWCNTをマウスへ咽頭吸引させた実験では，一過性の急性症状の後に，炎症性細胞浸潤を伴わない間質の繊維化が認められている.[12] また，ApoEノックアウトマウスを用いた実験では，タンパクカルボニル化活性の変化を伴うミトコンドリアDNA障害と，アテローム性動脈硬化症の進行を増強することが示された.[13] MWCNTに関しても，マウスにMWCNT（200–400 μg）を気管内滴下した実験では，一過性の肺の炎症反応に加え，投与量に依存した血小板の活性化と凝固作用の活性化の促進が示唆されている.[14] また，MWCNTやSWCNTの気管内投与や経鼻投与により，アレルギー反応の増強反応が報告されている.[15-17] これらの結果が，カーボンナノチューブが直接体内循環に侵入した結果であるか，免疫細胞との接触を介した反応であるかを区別することは難しいが，曝露局所に留まらない全身作用の可能性を示している．われわれの酸化チタンの気管内投与による発がんプロモーション作用が，炎症因子により介在されたことは，これらの知見と同様の作用様式を示すものととらえることもできる．

以上の知見は，短期の試験だけでは検証することは困難であり，ナノマテリアルの有害性を確認するためには，長期の体内動態予測や慢性影響に関する研究が，重要なステップであることを示している．Figure 4にスクリーニング試験や確定試験を開発するための手順についてまとめた．通常の化学物質については，その長い歴史の中で明らかとなった有害性に対して，それぞれの毒性発現様式に応じてスクリーニング試験が開発され，現在まで運用されてきている．特に変異原性試験は発がん性を予測する試験としての重要な役割を担っている．しかし，現時点ではナノマテリアルによる有害性影響が，これまでの研究経験の中で明らかとなった影響だけに留まるのかについては，まだ誰も判定できない状況である．これまでの一般化学物質に対応する有害性とスクリーニング試験を活用して進めていくと同時に，未知の影響を見極める最初のステップとして，少な

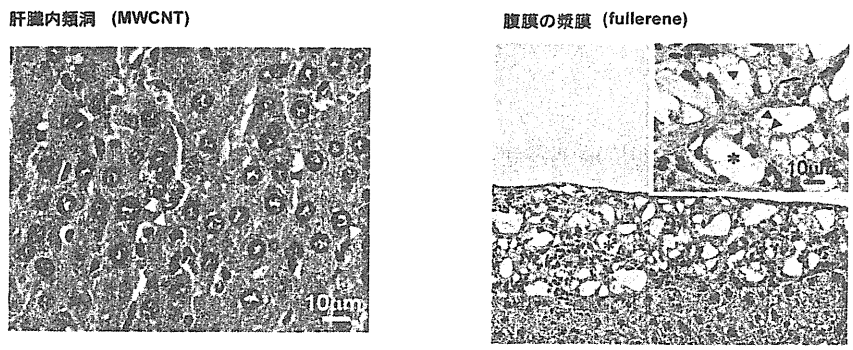

Fig. 3. The Suggestive Evidences for Systemic Toxicites by Nanomaterials

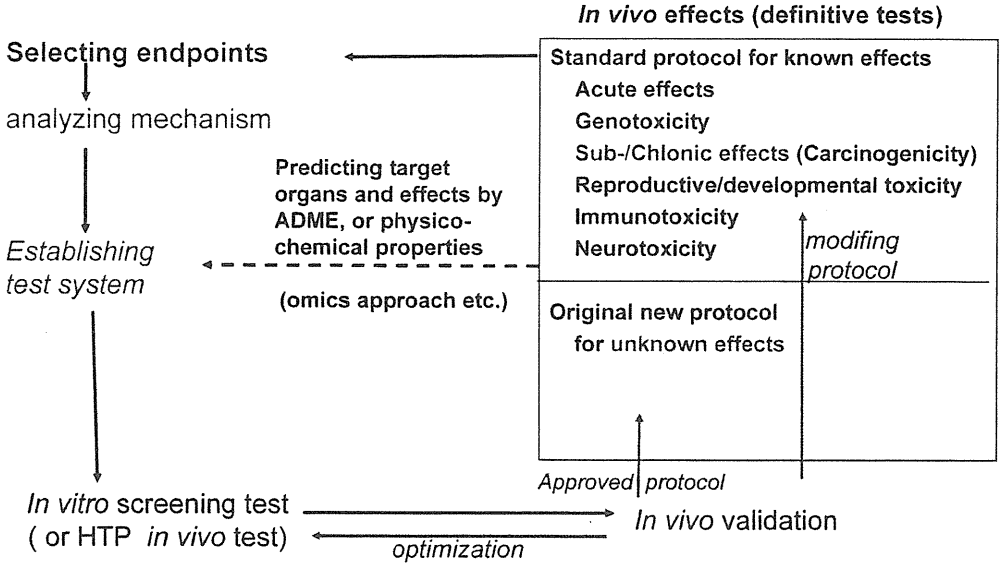

Fig. 4. The Schematic Development of Screening Tests and Definitive Tests

くとも代表的なナノマテリアルによる *in vivo* の慢性影響研究や，その影響を推定するためのナノマテリアルと生体成分との分子レベルでの相互作用や体内残留性様式の解析を進めていくべきであると考えられる．

謝辞　本稿で解説した研究成果の一部は，厚生労働科学研究費補助金（化学物質リスク研究事業）H17-化学-012，H18-化学一一般-007 及び H21-化学一一般-008 の助成によって行われたものです．

REFERENCES

1) Scientific Committee on Emerging and Newly Identified Health Risks, SCENIHR: ⟨http://ec.europa.eu/health/ph_risk/committees/04_scenihr/docs/scenihr_o_003b.pdf⟩, European Commission Web, cited 14 November, 2010.
2) Scientific Committee on Emerging and Newly Identified Health Risks, SCENIHR: ⟨http://ec.europa.eu/health/ph_risk/committees/04_scenihr/docs/scenihr_o_010.pdf⟩, European Commission Web, cited 14 November, 2010.
3) Food Safety Authority of Ireland, FSA, "The Relevance for Food Safety of Applications of Nanotechnology in Food and Feed Industries," Dublin, 2008.
4) UK Committees on Toxicity, Mutagenicity and Carcinogenicity of Chemicals in Food, Consumer Products and the Environment (COT, COM, COC): ⟨http://cot.food.gov.uk/pdfs/cotstatements2005nanomats.pdf⟩, COT Web, cited 14 November, 2010.
5) The Committee on Toxicity of Chemicals in Food, Consumer Products and the Environment: ⟨http://www.food.gov.uk/multimedia/pdfs/cotstatementnanomats200701.pdf⟩, cited 14 November, 2010.
6) Takagi A., Hirose A., Nishimura T., Fukumori N., Ogata A., Ohashi N., Kitajima S., Kanno J., *J. Toxicol. Sci.*, **33**, 105–116 (2008).
7) Sakamoto Y., Nakae D., Fukumori N., Tayama K., Maekawa A., Imai K., Hirose A., Nishimura T., Ohashi N., Ogata A., *J. Toxicol. Sci.*, **34**, 65–76 (2009).
8) Xu J., Futakuchi M., Iigo M., Fukamachi K., Alexander D. B., Shimizu H., Sakai Y., Tamano S., Furukawa F., Uchino T., Tokunaga H., Nishimura T., Hirose A., Kanno J., Tsuda H., *Carcinogenesis*, **31**, 927–935 (2010).
9) Wako K., Kotani Y., Hirose A., Doi T., Hamada S., *J. Toxicol. Sci.*, **35**, 437–446 (2010).
10) Nurkiewicz T. R., Porter D. W., Hubbs A. F., Stone S., Chen B. T., Frazer D. G., Boegehold M. A., Castranova V., *Toxicol. Sci.*, **110**, 191–203 (2009).
11) Ryman-Rasmussen J. P., Cesta M. F., Brody